Bioorganic Chemistry 92 (2019) 103109

Contents lists available at ScienceDirect

Bioorganic Chemistry

journal homepage: www.elsevier.com/locate/bioorg

New series of fused pyrazolopyridines: Synthesis, molecular modeling, antimicrobial, antiquorum-sensing and antitumor activities

N.S. El-Gohary[a,*], S.S. Hawas[a,b], M.T. Gabr[a,c], M.I. Shaaban[d], M.B. El-Ashmawy[a]

[a] Department of Medicinal Chemistry, Faculty of Pharmacy, Mansoura University, Mansoura 35516, Egypt
[b] Department of Pharmaceutical Chemistry, Faculty of Pharmacy, Horus University, New Damietta, Egypt
[c] Department of Chemistry, University of Iowa, Iowa City, IA 52242, USA
[d] Department of Microbiology, Faculty of Pharmacy, Mansoura University, Mansoura 35516, Egypt

ARTICLE INFO

Keywords:
Fused pyrazolopyridines
Antimicrobial
Antiquorum-sensing
Antitumor
DNA-binding
Topoisomerase IIβ
Molecular modeling

ABSTRACT

New series of fused pyrazolopyridines were prepared and assessed for antimicrobial, antiquorum-sensing and antitumor activities. Antimicrobial evaluation toward selected Gram-positive bacteria, Gram-negative bacteria and fungi indicated that 5-phenylpyrazolopyridotriazinone **4a** has good and broad-spectrum antimicrobial activity. In addition, 5-(4-chlorophenyl)pyrazolopyridotriazinone **4b** and 5-(4-(dimethylamino)phenyl)pyrazolopyridotriazinone **4c** exhibited good activity against the selected Gram-positive bacteria and *A. fumigatus*, whereas 5-amino-4-phenylpyrazolopyridopyrimidine **6a** demonstrated good activity against *B. cereus* and *P. aeruginosa*. Furthermore, 6-amino-5-imino-4-phenylpyrazolopyridopyrimidine **7a** and 6-amino-4-(4-chlorophenyl)-5-iminopyrazolopyridopyrimidine **7b** demonstrated promising activity against the tested Gram-negative bacteria and fungi, and moderate activity against Gram-positive bacteria. Antiquorum-sensing screening over *C. violaceum* illustrated that **4a, 6a** and **7a-c** have strong activity. *In vitro* antiproliferative assessment of the new derivatives against HepG2, HCT-116 and MCF-7 cancer cells revealed that **7a** is the most active analog against all tested cell lines. Likewise, 3,7-dimethyl-4-phenylpyrazolopyridopyrimidinone **2a** and 6-amino-4-(4-chlorophenyl)-5-iminopyrazolopyridopyrimidine **7b** manifested strong activity against all examined cell lines. *In vivo* antitumor testing of **2a**, **7a** and **7b** against EAC cells in mice indicated that **7a** has the highest activity. Cytotoxicity toward WI38 and WISH normal cells was also assessed and results assured that all of the investigated analogs have lower cytotoxicity than doxorubicin. DNA-binding affinity and topoisomerase IIβ inhibitory activity were evaluated, and results revealed that **5b, 7a** and **7b** bind strongly to DNA; in addition, **2a**, **4a**, **7a** and **7b** manifested higher topoisomerase IIβ inhibitory activity than that of doxorubicin. Analogs **5b**, **7a** and **7b** were docked into topoisomerase IIβ, and results indicated that **7a** and **7b** have the highest binding affinity toward topoisomerase IIβ. *In silico* simulation studies referred that most of the new analogs comply with the optimum needs for good oral absorption. Also, computational carcinogenicity evaluation was predicted.

1. Introduction

Excessive and random utilization of antibiotics in treatment of bacterial infections led to evolution of multiple drug resistant strains [1]. Antimicrobial resistance (AMR) threatens the efficacious therapy of an ever-growing range of microbial infections. AMR is a terrible menace to the public health, and it needs urgent control to save human health [2]. On the other hand, bacteria replicating within quorum-sensing (QS) mediated biofilms are the prime cause of most infectious diseases. Suppression of bacterial QS is an auspicious way to battle resistant bacterial infections [3]. Natural and synthetic compounds were proved to be efficient in inhibiting QS [4–14]. Thus, the existing research aimed in one part to obtain new antimicrobials with QS inhibitory effect.

On the other hand, cancer is one of the prime health worries. Various risk factors contribute to the development of cancer, including radiation, chemicals, viruses and others. Cancer is characterized by metastasis, where cancer cells spread from the primary origin into different sites of the body through lymph system or bloodstream. Metastasis is responsible for 90% of cancer deaths [15]. The most prevalent types of cancer remedies include surgery, radiotherapy, chemotherapy and others. A typical anticancer agent should selectively target cancer cells without impairing normal ones. Over the years, cancer is still a master field of investigation, and medicinal chemistry

* Corresponding author.
E-mail addresses: dr.nadiaelgohary@yahoo.com, el_gohary@mans.edu.eg (N.S. El-Gohary).

https://doi.org/10.1016/j.bioorg.2019.103109
Received 29 December 2018; Received in revised form 2 July 2019; Accepted 4 July 2019
Available online 06 July 2019
0045-2068/

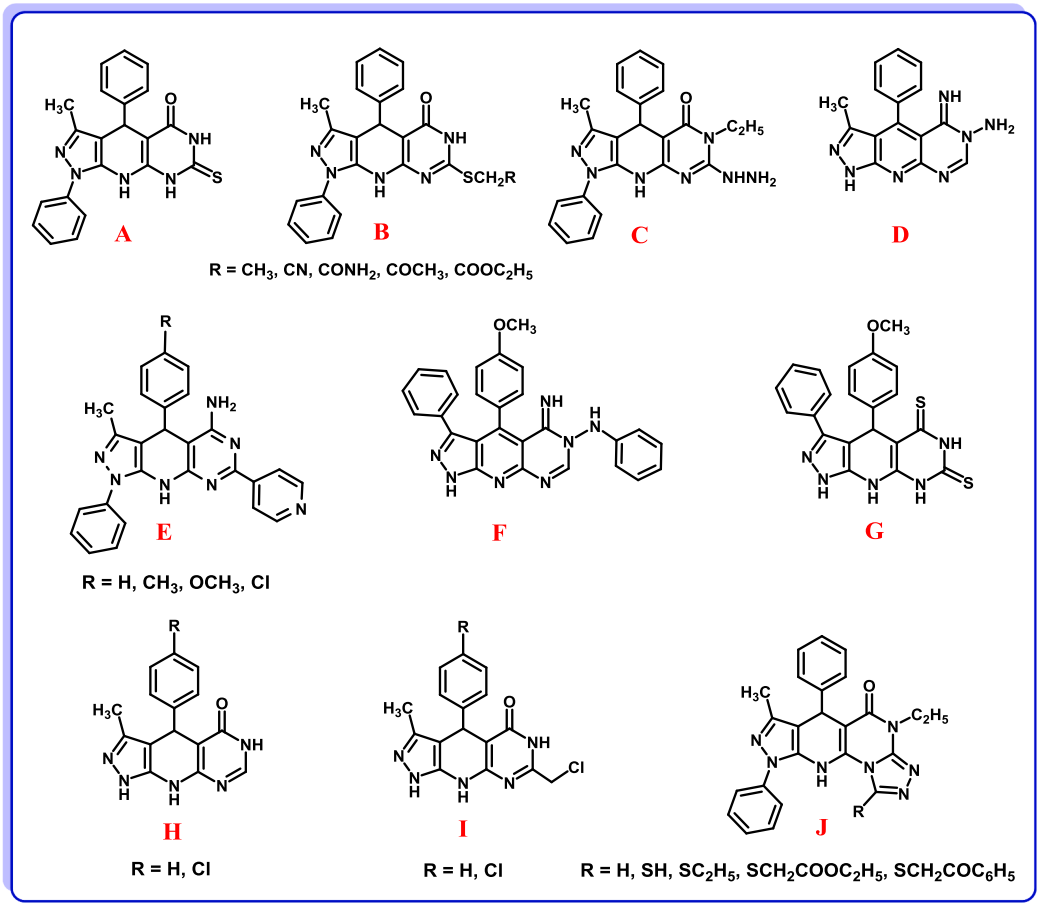

Fig. 1. Examples of pyrazolo[4′,3′:5,6]pyrido[2,3-*d*]pyrimidines with reported antimicrobial **(A-C)**, antibacterial **(D)**, antifungal **(E)** and antitumor **(F-I)** activities, and pyrazolo[4′,3′:5,6]pyrido[3,2-*e*][1,2,4]triazolo[4,3-*a*]pyrimidinones **(J)** with reported antibacterial activity.

researchers are keen in design and evolution of new potent and selective anticancer agents. DNA topoisomerases (TOP I, IIα and IIβ) encompass a prime aspect of basic cellular biology, and they are considered as good targets for various antibacterial [16] and anticancer agents [16,17]. TOP IIβ inhibitors act by prohibiting the TOP enzyme from relinking DNA strands after cleavage and transform topoisomerases into DNA detrimental agents [18]. Although drugs of diversified classes that act by various mechanisms are available, there are some troubles linked with the currently available drugs. Therefore, researchers are interested in designing, synthesizing and evaluating various new bioactive molecules targeting topoisomerases.

Pyrazolo[3,4-*b*]pyridine nucleus is an important scaffold for synthesis of lots of bioactive compounds [4–6,19,20]. Pyrazolopyridopyrimidine analogs were reported to have diverse pharmacological activities, including antibacterial [21–23], antifungal [24], antimicrobial [25,26] and antitumor [22,27,28] activities. For example, pyrazolopyridopyrimidines **A-C** [26] (Fig. 1) were proved to have broad-spectrum antimicrobial activity, while **D** [25] (Fig. 1) was found to have good antibacterial activity. In addition, compounds **E** [24] (Fig. 1) exhibited antifungal activity. On the other hand, pyrazolopyridopyrimidines **F** [27], **G** [27], **H** [28] and **I** [28] (Fig. 1) demonstrated promising antitumor activity; in addition, **F** [27] and **G** [27] were reported to have strong DNA-binding affinity. Further, pyrazolo[4′,3′:5,6]pyrido[3,2-*e*][1,2,4]triazolo[4,3-*a*]pyrimidinone analogs **J** [26] (Fig. 1) were reported as antimicrobial agents.

1.1. Rational design

Depending on the literature findings, pyrazolo[3,4-*b*]pyridine derivatives **K** [4], **L** [5] and **M** [6] (Fig. 2) were described as promising antimicrobial and antitumor agents. Further, the pyrimidine derivatives **N** [29] (Fig. 2) were reported to have antimicrobial and antitumor activities. Moreover, [1,2,4]triazole derivatives **O, P** [30,31] and **Q** [32] (Fig. 2) were described as antimicrobial and antitumor agents, respectively.

Molecular hybridization is a promising strategy for preparation of new active compounds, and it is widely used in medicinal chemistry. Hybridization of two active molecules with dissimilar pharmacophores led to enhanced activities [33,34]. Promoted by these literature findings, we found it motivating to design new series of pyrazolopyridopyrimidine hybrids **2a-c, 3c, 6a-c** and **7a-c** combining pyrazolopyridine and pyrimidine pharmacophores (Fig. 2), and two series of pyrazolo[4′,3′:5,6]pyrido[3,2-*e*][1,2,4]triazolo[1,5-*c*]pyrimidine hybrids **8a,c** and **9a-c** combining pyrazolopyridopyrimidine and [1,2,4]triazole pharmacophores (Fig. 2). On the other hand, fused [1,2,3]triazines **R** [35] (Fig. 3) were reported to have antimicrobial activity, whereas **S** [36] and **T** [37] (Fig. 3) were evidenced to have antitumor activity. Therefore, we found it interesting to prepare a new series of pyrazolopyridotriazinone hybrids **4a-c** combining pyrazolopyridine and [1,2,3]triazine pharmacophores (Fig. 3). The designed new series of compounds **2–9** were synthesized and examined for antimicrobial and antitumor activities. The active antimicrobial and/or antitumor analogs, **2a, 4a-c, 5b, 6a, 7a** and **7b** were valued for DNA-binding affinity and TOP IIβ inhibitory effect to find out their probable mode of action. Detailed analysis of structure-activity correlation of the new fused pyrazolopyridines will pave the road for synthesis and evolution of new more active derivatives.

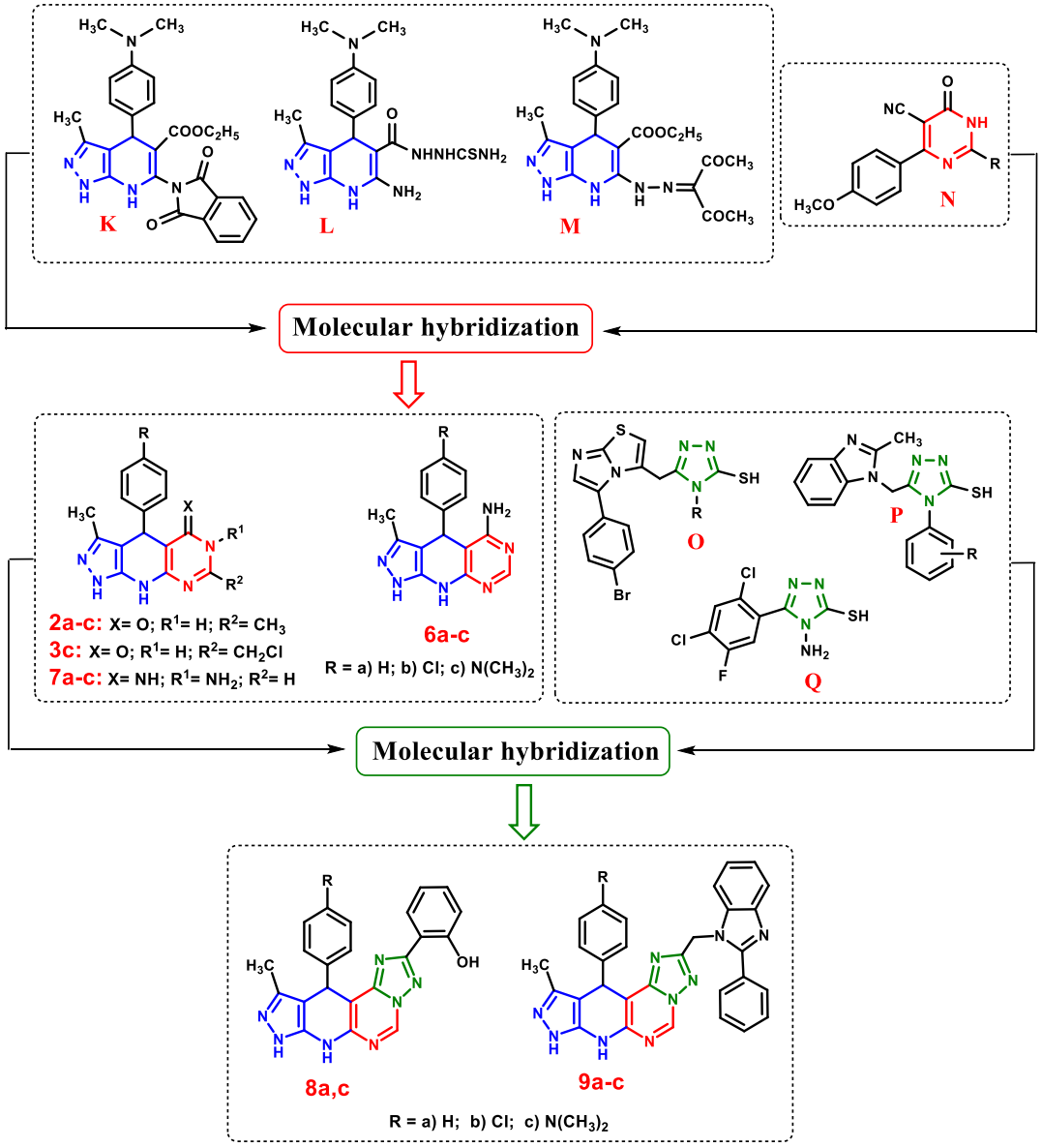

Fig. 2. The designed new hybrids **2a-c**, **3c**, **6a-c**, **7a-c**, **8a,c** and **9a-c** as potential antimicrobial and antitumor agents.

2. Results and discussion

2.1. Chemistry

Synthesis of the new fused pyrazolopyridines **2–9** has been performed starting with 6-aminopyrazolopyridine-5-carbonitriles **1a-c** [28] (Schemes 1 and 2).

Pointing to Scheme 1, refluxing **1a-c** with glacial acetic acid in the presence of concentrated HCl gave 3,7-dimethylpyrazolopyridopyrimidinones **2a-c**. The reaction proceeds *via* conversion of nitrile group into amide that was subsequently cyclized *via* Dimorth rearrangement to furnish the pyrazolopyridopyrimidines [38,39]. Heating **1c** with chloroacetyl chloride in dimethylformamide (DMF) gave 7-chloromethylpyrazolopyridopyrimidinone **3c**. The pyrazolopyridotriazinones **4a-c** were synthesized by diazotization of **1a-c** *via* treating with aqueous sodium nitrite and a mixture of HCl/glacial acetic acid (3:1). Referring to Scheme 2, condensation of **1a-c** with triethyl orthoformate gave the ethyl formimidates **5a-c**. Reaction of ethyl formimidates **5a-c** with ammonia 35% in refluxing ethanol gave 5-aminopyrazolopyridopyrimidines **6a-c**. Heating **5a-c** with hydrazine hydrate in ethanol yielded 6-amino-5-iminopyrazolopyridopyrimidines **7a-c**. Interaction of **5a-c** with 2-hydroxybenzohydrazide or 2-(2-phenyl-1*H*-benzimidazol-1-yl)acetohydrazide in refluxing DMF gave the pyrazolopyridotriazolopyrimidines **8a,c** and **9a-c**, respectively. The structures of the new analogs were assured by spectral and elemental analyses.

2.2. Biology

2.2.1. Antimicrobial and antiquorum-sensing screening

The new derivatives **2–9** were examined for antibacterial activity toward selected resistant Gram-positive bacteria (*Staphylococcus aureus* ATCC 29213 and *Bacillus cereus* UW 85) and Gram-negative bacteria (*Escherichia coli* ATCC 12435 and *Pseudomonas aeruginosa*) [11,12,40]. Antifungal screening toward *Candida albicans* (clinical isolate) and *Aspergillus fumigatus* 293 was also carried out [11,12,41,42]. Inhibition zone diameters (mm) (Table 1) and minimal inhibitory concentrations (MICs, μg/mL and μM) (Table 2) of the tested analogs over the chosen microorganisms were determined. Ciprofloxacin, ampicillin and fluconazole were employed as reference drugs. Results illustrated that **4a** has good and broad-spectrum antimicrobial activity (MIC = 39.06–312.5 μg/mL). Compounds **2b** and **2c** manifested

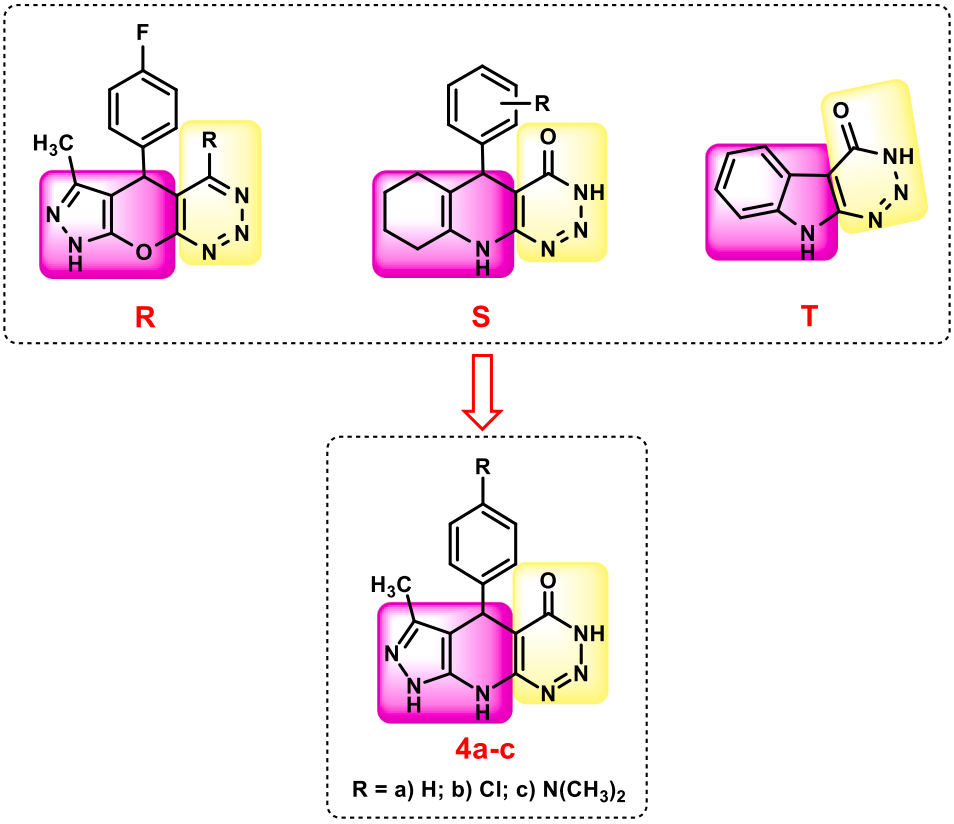

Fig. 3. Reported fused [1,2,3]triazines with antimicrobial (**R**) and antitumor (**S,T**) activities, and the proposed pyrazolo[4′,3′:5,6]pyrido[2,3-*d*][1,2,3]triazin-4-ones **4a-c** with expected antimicrobial and antitumor activities.

moderate activity on *B. cereus* (MIC = 312.5 μg/mL), whereas compound **3c** showed good activity on *B. cereus* (MIC = 156.25 μg/mL), and moderate activity on *P. aeruginosa* (MIC = 312.5 μg/mL). Moreover, **4b** showed good activity on *S. aureus*, *A. fumigatus* (MIC = 78.125 μg/mL) and *B. cereus* (MIC = 156.25 μg/mL), whereas **4c** manifested good activity against *B. cereus* and *A. fumigatus* (MIC = 78.125 μg/mL), and moderate activity toward *S. aureus* (MIC = 312.5 μg/mL). Compound **6a** evinced good activity on *B. cereus* (MIC = 78.125 μg/mL) and *P. aeruginosa* (MIC = 156.25 μg/mL). On the other hand, **7a** exhibited good activity on Gram-negative bacteria and the two selected fungi (MIC = 156.25 μg/mL), and moderate activity on Gram-positive bacteria (MIC = 625 μg/mL). As well, **7b** demonstrated good activity on the tested Gram-negative bacteria and fungi (MIC = 39.06–78.125 μg/mL), and moderate activity on the tested Gram-positive bacteria (MIC = 625 μg/mL). Further, **8a** illustrated moderate activity on Gram-positive bacteria (MIC = 312.5 μg/mL). The rest of the tested compounds were evidenced to be weakly active or inactive against the selected microbes.

QS inhibitory activity of the synthesized analogs over *Chromobacterium violaceum* ATCC 12472 was valued [11,12,43] utilizing indole as a comparative compound.

QS system of *C. violaceum* releases signals that monitor the emancipation of the violet pigment (violacein) that could be utilized to establish QS communication between bacteria [44,45]. Consequently, inhibition of QS activity in *C. violaceum* will stop the liberation of violacein. Anti-QS activity was estimated by subtracting radius of bacterial growth inhibition (r_1) from the whole radius of growth and pigment inhibition (r_2), QS inhibition = (r_2-r_1) in mm. Derivatives **4a, 6a** and **7a-c** demonstrated strong anti-QS activity (radius of pigment inhibition = 17–24 mm), and the five analogs were proved to be more active than indole (radius of pigment inhibition = 15 mm) and the previously prepared anti-QS compounds [4–12]. On the other hand, **2a** was moderately active (radius of pigment inhibition = 14 mm) (Table 1).

2.2.1.1. Structure-activity correlation

*2.2.1.1.1. Regarding analogs **2a-c, 3c** and **4a-c**.* Compound **2a** showed moderate anti-QS activity with no antimicrobial activity toward all tested microbial strains, whereas pyrazolopyridopyrimidines **2b** and **2c** demonstrated moderate activity on *B. cereus*, and abolished anti-QS activity, and this could be explained by increased lipophilicity of **2b** and **2c** (logP = 2.54 and 1.96, respectively) compared to **2a** (logP = 1.86). Further, exchanging 7-methyl substituent in **2c** with 7-chloromethyl counterpart led to better activity against *B. cereus* and *P. aeruginosa* (compound **3c**), and this might be attributed to increased lipophilicity of **3c** (logP = 2.56) compared to **2c** (logP = 1.96). Presence of (unsubstituted phenyl) moiety at 5-position of pyrazolopyridotriazine nucleus led to promising antifungal activity over both of the tested fungi, good antibacterial activity over the four tested bacteria, and strong anti-QS activity (analog **4a**). Replacing 5-(unsubstituted phenyl) in **4a** with 5-(4-chlorophenyl) led to increased activity toward *S. aureus*, decreased activity toward *A. fumigatus*, and abolished activity toward the tested Gram-negative bacteria and *C. albicans*, as well as abolished anti-QS activity (compound **4b**), whereas its exchange with 5-(4-(dimethylamino)phenyl) resulted in increased activity toward *B. cereus*, lowered activity toward *S. aureus* and *A. fumigatus*, and abolished activity toward *E. coli*, *P. aeruginosa* and *C. albicans*, as well as abolished anti-QS activity (compound **4c**). The strong anti-QS activity of **4a** compared to **4b** and **4c** might be attributed to decreased lipophilicity of **4a** (logP = 1.63) compared to **4b** and **4c** (logP = 2.31 and 1.73, respectively).

*2.2.1.1.2. Referring to compounds **5a-c, 6a-c** and **7a-c**.* The pyrazolopyridines **5a-c** showed neither antimicrobial nor anti-QS activity. The antibacterial activity toward *B. cereus* and *P. aeruginosa*, and the anti-QS activity of compounds **6a-c** are reliant on the type of

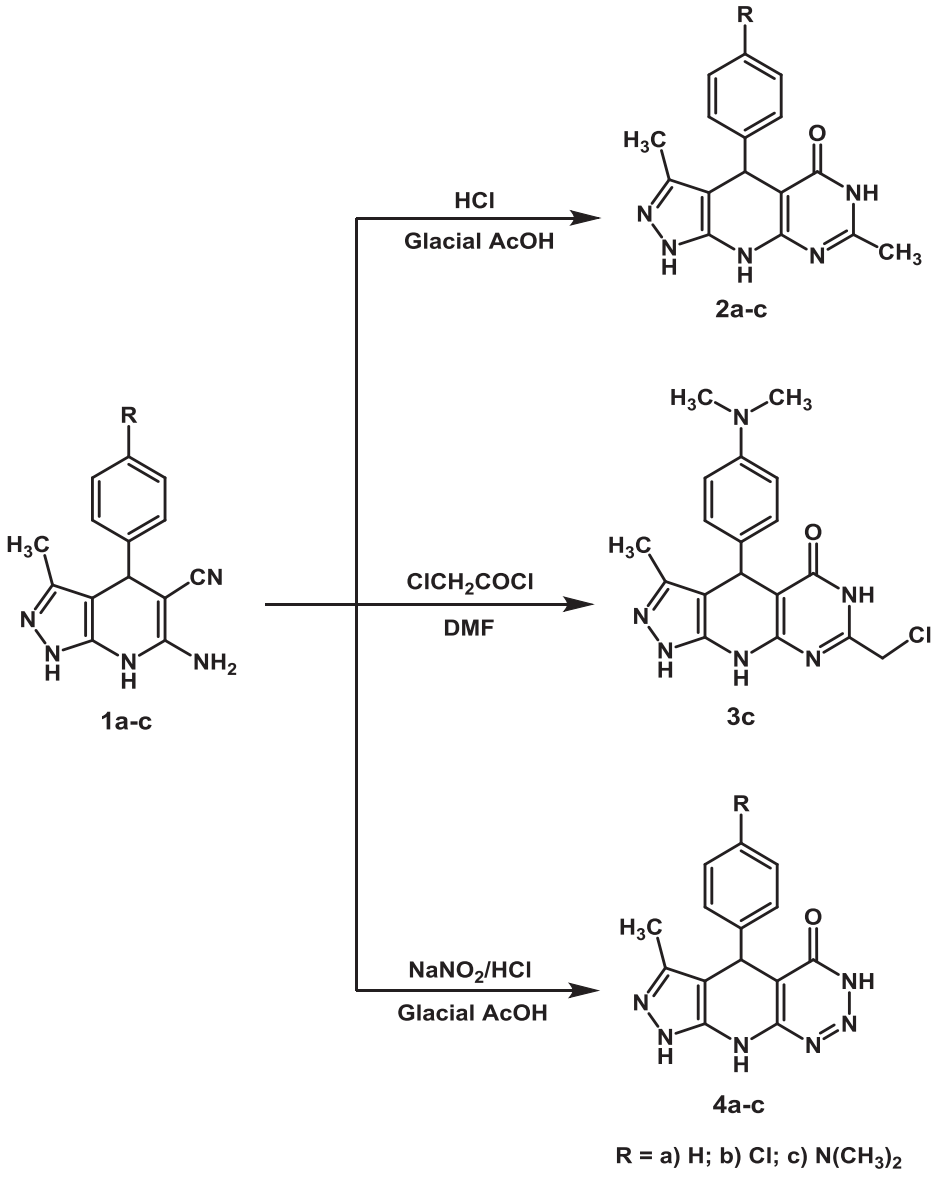

Scheme 1. Synthesis of compounds **2–4.**

substituent at 4-position of pyrazolopyridopyrimidine skeleton, whereas introduction of 4-(unsubstituted phenyl) moiety led to good activity toward both bacterial strains, and strong anti-QS activity (compound **6a**). Replacement of 4-(unsubstituted phenyl) with 4-(4-chlorophenyl) led to decreased effect against both bacterial strains, and abolished anti-QS activity (compound **6b** versus **6a**). On the other hand, exchanging 4-(unsubstituted phenyl) with 4-(4-(dimethylamino) phenyl) resulted in abolished activity toward all tested strains, and abolished anti-QS activity (compound **6c** versus **6a**). The increased anti-QS activity of **6a** might be due to its decreased lipophilicity (logP = 1.93) compared to **6b** and **6c** (logP = 2.61 and 2.03, respectively). The 6-amino-5-imino-4-phenylpyrazolopyridopyrimidine analog **7a** exhibited obvious activity over Gram-negative bacteria and the two selected fungi, and moderate activity over Gram-positive bacteria. Replacing 4-(unsubstituted phenyl) in **7a** with 4-(4-chlorophenyl) led to enhanced effectiveness on the chosen Gram-negative bacteria and fungi (compound **7b**), whereas its exchange with 4-(4-(dimethylamino)phenyl) led to retained effectiveness on *P. aeruginosa*, and diminished activity over other examined microbes (compound **7c**). On the other hand, the 6-amino-5-imino-4-((un)substituted phenyl)pyrazolopyridopyrimidine analogs **7a-c** exhibited strong anti-QS activity that might be attributed to their decreased lipophilicity (logP = 0.12, 0.8 and 0.23, respectively), and presence of additional hydrogen bond donor sites.

*2.2.1.1.3. With respect to compounds **8a,c** and **9a-c**.* The 11-phenyl-2-(2-hydroxyphenyl)pyrazolopyridotriazolopyrimidine analog **8a** has moderate activity over Gram-positive bacteria. Replacing 11-(unsubstituted phenyl) in **8a** with 11-(4-(dimethylamino)phenyl) led to revoked activity over all tested microbes (compound **8c**). In addition, replacing 2-(2-hydroxyphenyl) substituent with 2-((2-phenyl-1*H*-benzimidazol-1-yl)methyl) counterpart regardless of the type of 11-substituent led to revoked activity over all screened microbes (compounds **9a-c**). On the other hand, the 11-((un)substituted phenyl)-2-substituted-pyrazolopyridotriazolopyrimidine analogs **8a,c** and **9a-c** showed no anti-QS activity.

2.2.2. Antitumor testing

2.2.2.1. In vitro antiproliferative screening. Antiproliferative activity of the new derivatives against HepG2 liver, HCT-116 colon and MCF-7 breast cancer cells was estimated in accord to MTT assay, and utilizing doxorubicin as a reference agent [46–48]. The concentration of compound that prohibits viability of cells by 50% (IC_{50}, μM) was

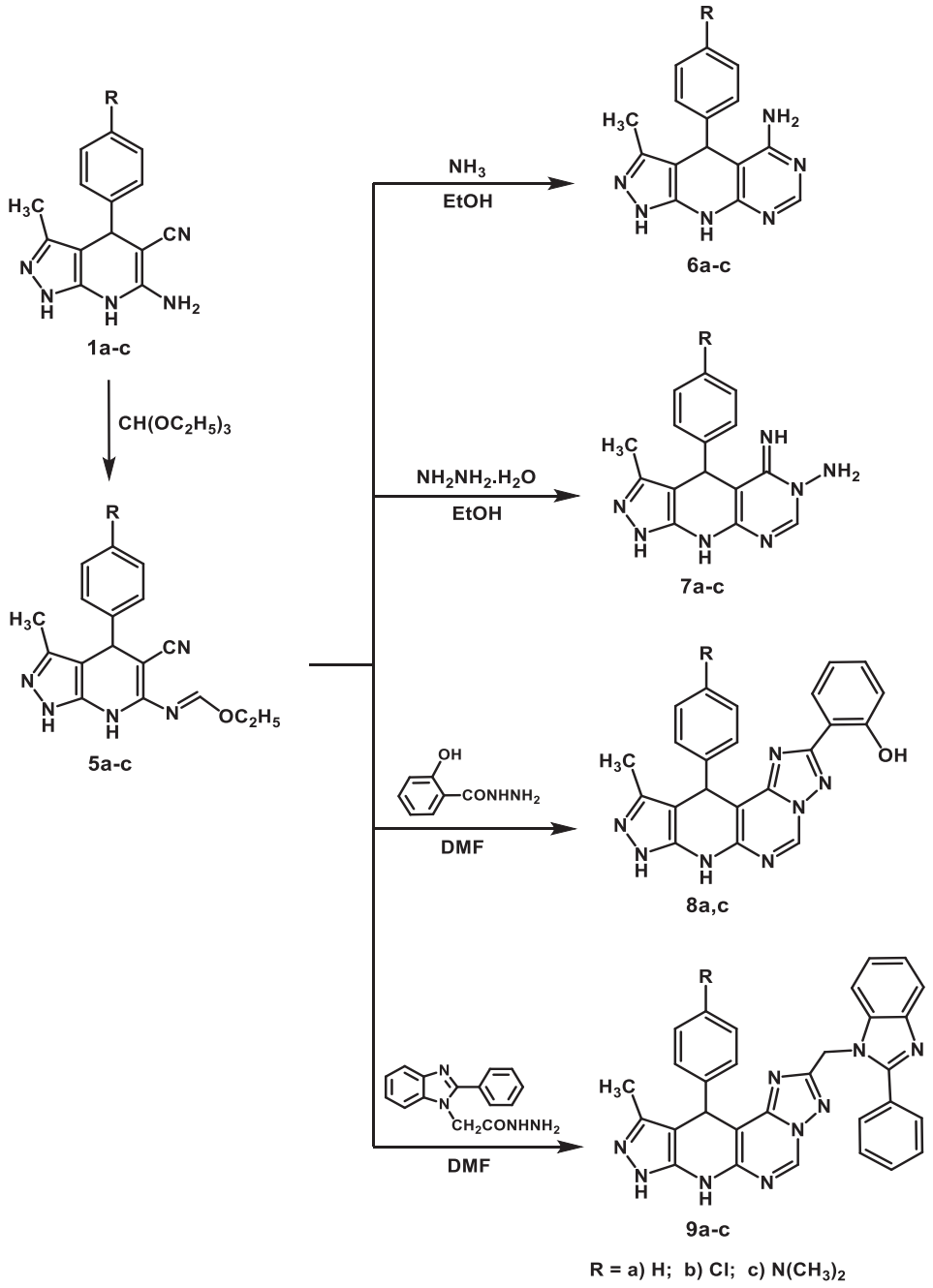

Scheme 2. Synthesis of compounds **5–9.**

calculated. Analog **7a** showed the highest activity on all tested cell lines (IC_{50} = 3.18–5.79 μM), and this analog was proved to be more potent than the previously prepared pyrazolopyridopyrimidines **F** [27] and **G** [27] toward the three selected cell lines (IC_{50} = 7.80–14.60 μM). As well, **2a, 5b** and **7b** demonstrated strong activity over all examined cell lines (IC_{50} = 8.87–15.97 μM) though less than that of doxorubicin (IC_{50} = 4.17–5.23 μM). On the other hand, compounds **3c**, **5c**, **6c** and **7c** exhibited moderate activity toward all tested cell lines (IC_{50} = 22.61–49.86 μM), whereas **5a**, **6b** and **8a** displayed moderate activity toward HCT-116 and MCF-7 cancer cells (IC_{50} = 38.08–49.27 μM). Further, **2b** and **9c** exhibited moderate activity over MCF-7 cells with IC_{50} values of 45.69 and 48.91, respectively. The remaining analogs manifested weak or no activity toward the screened cell lines (Table 3).

2.2.2.1.1. Structure-activity correlation

*2.2.2.1.1.1. Regarding analogs **2a-c**, **3c** and **4a-c***

The 4-phenylpyrazolopyridopyrimidinone **2a** exhibited strong antiproliferative activity against all examined cell lines. Exchanging 4-(unsubstituted phenyl) in **2a** with 4-(4-chlorophenyl) or 4-(4-(dimethylamino)phenyl) led to decreased activity against all examined cell lines (analogs **2b** and **2c**). On contrary, replacing 7-methyl substituent in **2c** with 7-chloromethyl boosted the activity against the three cancer cells (analog **3c** versus **2c**), and this might be attributed to increased lipophilicity of **3c** (logP = 2.56) compared to **2c** (logP = 1.96). Introduction of 5-(unsubstituted phenyl) moiety into the pyrazolopyridotriazine nucleus produced **4a** with weak effectiveness on the three chosen cell lines. Exchanging 5-(unsubstituted phenyl) with 5-(4-chlorophenyl) or 5-(4-(dimethylamino)phenyl) led to reduced effect over all examined cell lines (analogs **4b** and **4c** versus **4a**).

Table 1
Antimicrobial and antiquorum-sensing testing results.

Comp. No.	Inhibition zone diameter (mm)[a]						QS inhibition (mm)[a]
	S. aureus	*B. cereus*	*E. coli*	*P. aeruginosa*	*C. albicans*	*A. fumigatus*	*C. violaceum*
2a	–	–	–	–	–	–	14
2b	**–**	**19**	–	–	–	–	–
2c	–	**19**	**–**	**–**	–	**–**	–
3c	–	**23**	–	**18**	–	–	–
4a	**19**	**21**	14	**19**	**26**	**29**	**18**
4b	**23**	**21**	**–**	**–**	–	**26**	–
4c	**17**	**26**	–	–	–	**23**	–
5a	–	–	–	–	–	–	–
5b	–	–	–	–	–	–	–
5c	–	–	–	–	–	–	–
6a	–	**22**	–	**21**	–	–	**24**
6b	–	13	–	10	–	–	**–**
6c	–	**–**	–	–	–	–	**–**
7a	11	15	**20**	**21**	**21**	**19**	**19**
7b	11	13	**27**	**25**	**25**	**32**	**17**
7c	–	–	–	**23**	–	–	**19**
8a	**19**	**18**	–	–	–	–	–
8c	–	–	–	–	–	**–**	–
9a	–	–	–	–	–	**–**	–
9b	–	–	–	–	–	**–**	–
9c	–	–	–	–	–	–	–
Ciprofloxacin	30	35	30	40	–	–	–
Ampicillin	18	15	23	18	na	na	na
Fluconazole	na	na	na	na	11	11	na
Indole	na	na	na	na	na	na	15

[a] Inhibition zone diameter (mm) and QS inhibition (mm): no activity (−, < 2); weak (2–9); moderate (10–15); strong (15–25); very strong (> 25).
na: not assigned.
Bold values shed light on the preferable results.

*2.2.2.1.1.2. Referring to compounds **5a-c, 6a-c** and **7a-c***

The activity of pyrazolopyridines **5a-c** is reliant on the type of 4-substituent, whereas existence of 4-(4-chlorophenyl) substituent led to higher activity than the 4-(unsubstituted phenyl) and 4-(4-(dimethylamino)phenyl) counterparts (compound **5b** versus **5a** and **5c**), and this might be due to boosted lipophilicity of **5b** (logP = 2.08) comparable to **5a** and **5c** (logP = 1.40 and 1.50, respectively), the activity order is **5b** > **5c** > **5a**. The sensitivity of the three cancer cell lines to derivatives **6a-c** is reliant on the type of substituent at 4-position of pyrazolopyridopyrimidine skeleton, whereas existence of 4-(4-(dimethylamino)phenyl) moiety led to stronger efficacy toward all tested cancer cells than the 4-(unsubstituted phenyl) and 4-(4-chlorophenyl) counterparts (compound **6c** versus **6a** and **6b**), the activity order is **6c** > **6b** > **6a**. The type of 4-substituent on the pyrazolopyridopyrimidine skeleton affects the antiproliferative activity of compounds **7a-c**, whereas existence of 4-(unsubstituted phenyl) moiety resulted in higher activity toward the three cell lines than the 4-(4-chlorophenyl) and 4-(4-(dimethylamino)phenyl) counterparts (compound **7a** versus **7b** and **7c**), the activity order is **7a** > **7b** > **7c**. Moreover, existence of electron-withdrawing substituent at 4-position of phenyl ring ensures higher activity than the electron-donating counterpart (**7b** versus **7c**).

Table 2
MICs of the efficacious compounds.

Comp. No.	MIC μg/mL (μM)[a,b]					
	S. aureus	*B. cereus*	*E. coli*	*P. aeruginosa*	*C. albicans*	*A. fumigatus*
2b	**–**	312.5 (953.41)	–	–	–	–
2c	–	312.5 (928.95)	–	**–**	–	**–**
3c	–	**156.25 (421.34)**	–	312.5 (842.68)	–	–
4a	**156.25 (557.46)**	**156.25 (557.46)**	312.5 (1114.92)	**156.25 (557.46)**	**78.125 (278.73)**	**39.06 (139.36)**
4b	**78.125 (248.23)**	**156.25 (496.46)**	–	**–**	**–**	**78.125 (248.23)**
4c	312.5 (966.41)	**78.125 (241.60)**	–	–	**–**	**78.125 (241.60)**
6a	–	**78.125 (280.70)**	**–**	**156.25 (561.40)**	–	–
6b	–	625 (1998.34)	–	625 (1998.34)	–	–
7a	625 (2130.72)	625 (2130.72)	**156.25 (532.68)**	**156.25 (532.68)**	**156.25 (532.68)**	**156.25 (532.68)**
7b	625 (1906.72)	625 (1906.72)	**78.125 (238.34)**	**78.125 (238.34)**	**78.125 (238.34)**	**39.06 (119.17)**
7c	–	–	–	**156.25 (464.47)**	–	–
8a	312.5 (790.28)	312.5 (790.28)	–	–	–	–
Ciprofloxacin	19.53 (58.94)	19.53 (58.94)	19.53 (58.94)	< 9.76 (29.46)	na	na
Ampicillin	78.125 (213.81)	312.5 (855.23)	9.76 (26.71)	156.25 (427.61)	na	na
Fluconazole	na	na	na	na	1250 (4081.35)	2500 (8162.70)

[a] MIC > 2500 μg/mL.
[b] MICs (μM) are demonstrated between parentheses.
na: not assigned.
Bold values shed light on the preferable results.

Table 3
In vitro antiproliferative testing results.

Comp. No.	IC_{50} (μM)[a,b]		
	HepG2	HCT-116	MCF-7
2a	**10.04 ± 1.7**	**10.70 ± 1.8**	**8.87 ± 1.3**
2b	59.91 ± 3.5	62.84 ± 3.6	45.69 ± 2.9
2c	73.29 ± 4.1	69.52 ± 4.2	59.23 ± 3.6
3c	44.82 ± 3.1	41.01 ± 2.8	31.38 ± 2.4
4a	72.87 ± 5.2	72.49 ± 5.1	61.97 ± 4.5
4b	> 100.00	93.73 ± 5.5	90.34 ± 4.9
4c	> 100.00	> 100.00	94.60 ± 5.4
5a	57.24 ± 3.5	47.12 ± 3.0	38.08 ± 2.5
5b	**15.97 ± 2.5**	**14.09 ± 2.0**	**15.43 ± 1.9**
5c	49.86 ± 3.1	36.75 ± 2.7	33.50 ± 2.3
6a	67.29 ± 3.9	63.49 ± 3.7	53.85 ± 3.3
6b	61.29 ± 3.6	43.60 ± 2.9	49.27 ± 3.0
6c	32.47 ± 2.4	39.23 ± 2.7	22.61 ± 1.7
7a	**5.34 ± 0.5**	**3.18 ± 0.2**	**5.79 ± 0.6**
7b	**8.99 ± 0.9**	**9.77 ± 1.1**	**9.46 ± 1.0**
7c	32.03 ± 2.7	27.11 ± 2.3	28.33 ± 2.0
8a	50.87 ± 3.3	45.16 ± 3.4	40.37 ± 2.7
8c	83.32 ± 4.7	77.23 ± 4.5	74.28 ± 4.1
9a	95.71 ± 5.6	> 100.00	> 100.00
9b	86.45 ± 4.8	81.36 ± 4.6	81.53 ± 4.7
9c	58.26 ± 3.5	52.91 ± 3.3	48.91 ± 2.8
Doxorubicin	4.50 ± 0.2	5.23 ± 0.3	4.17 ± 0.2

[a] IC_{50} values = mean ± SD of three readings.
[b] IC_{50} (μM): strong (1–20); moderate (21–50); weak (51–100); no activity (> 100).
Bold values shed light on the preferable results.

*2.2.2.1.1.3. With respect to compounds **8a,c** and **9a-c***

The 11-phenyl-2-(2-hydroxyphenyl)pyrazolopyridotriazolopyrimidine analog **8a** has moderate activity on all examined cell lines. Replacing 11-(unsubstituted phenyl) in **8a** with 11-(4-(dimethylamino)phenyl) counterpart led to decreased effect toward all examined cells (analog **8c**). Furthermore, exchanging 2-(2-hydroxyphenyl) substituent in **8c** with 2-((2-phenylbenzimidazol-1-yl)methyl) resulted in increased activity on all screened cancer cells (derivative **9c**). On contrary, exchanging 4-(4-(dimethylamino)phenyl) substituent in **9c** with 4-(unsubstituted phenyl) or 4-(4-chlorophenyl) led to decreased effect toward all examined cells (analogs **9a** and **9b**, respectively).

2.2.2.2. In vivo antitumor screening. *In vivo* antitumor activity of **2a, 7a** and **7b** toward Ehrlich ascites carcinoma (EAC) in mice was esteemed [49–51]. Mean survival time (MST) and % increase in lifespan (% ILS) were calculated (Table 4) and (Fig. 4), whereas analogs **2a, 7a** and **7b** exhibited salient ILS of mice bearing EAC. Tumor parameters (viable tumor cell count and tumor volume) were assessed (Table 5) and (Fig. 5), where **7a** displayed conspicuous decrease in tumor cell count and tumor volume. Hematological parameters were assessed, and results (Table 6) and (Fig. 6) evinced that **7a** and **7b** have higher hemoglobin (Hb) and red blood cells (RBCs) levels and lower white blood cells (WBCs) count than doxorubicin (reference agent).

Table 4
Influence of **2a**, **7a** and **7b** on MST and % ILS of mice carrying EAC.

Group	MST (day)[a]	% ILS[a]
Normal	na	na
EAC only	16	na
2a	51	218.75
7a	**66**	**312.50**
7b	55	243.75
Doxorubicin	57	256.25

[a] Results are the mean of three readings.
na: not assigned.
Bold values shed light on the preferable results.

2.2.2.3. In vitro cytotoxicity screening against normal cells. Cytotoxicity of **2a, 7a** and **7b** over WI38 lung fibroblast and WISH amnion epithelial normal cells was estimated in comparison to doxorubicin (standard drug) [46–48], and IC_{50} values (μM) were assigned (Table 7). The tested analogs manifested lower cytotoxicity (IC_{50} = 11.81–63.41 μM) than doxorubicin (IC_{50} = 6.68–8.14 μM), and they were proved to be safe toward the examined normal cells at their cytotoxic concentrations over the tested cancer cells.

2.2.3. Mechanistic studies

2.2.3.1. DNA-binding assay. DNA is the biological target for various antimicrobial and antitumor drugs [52]. Therefore, the efficacious compounds in the current study were evaluated for DNA-binding affinity following methyl green/DNA displacement assay [53].

Methyl green/DNA displacement assay [53] is used for evaluating the displacement of methyl green from DNA by compounds that bind to DNA. Concentrations of analogs **2a, 4a-c, 5b, 6a, 7a, 7b** and doxorubicin (DNA intercalator) that lowers absorbance of methyl green/DNA complex by 50% (IC_{50}, μM) were determined (Table 8). Studying the results, it was found that **5b, 7a** and **7b** bind strongly to DNA with IC_{50} values of 27.16, 35.12 and 36.20 μM, respectively, and the three derivatives are expected to act through binding to DNA. Besides, the three derivatives were proved to have better affinity than the previously synthesized pyrazolopyridopyrimidines **F** [27] and **G** [27] with IC_{50} values of 45.21 and 42.31 μM, respectively. Moreover, **2a** and **4a** exhibited moderate affinity with IC_{50} values of 42.39 and 43.35 μM, respectively, whereas **4b, 4c** and **6a** demonstrated weak affinity with IC_{50} values of 82.38, 59.03 and 63.47 μM, respectively.

2.2.3.2. Topoisomerase IIβ inhibition assay. In order to interpret the distinguished antimicrobial and antiproliferative activities of the new compounds, TOP IIβ was selected to assess the enzyme inhibitory activity of the active compounds in the current research. This enzyme is well recognized as a target for antibacterial [16] and anticancer agents [16,17].

TOP IIβ inhibitory activity of the most active compounds, **2a, 4a-c, 5b, 6a, 7a, 7b** and doxorubicin (positive control) was evaluated [54], and results are shown in Table 9. Analogs **2a, 4a, 7a** and **7b** showed strong TOP IIβ inhibitory activity (IC_{50} = 0.355, 0.433, 0.314 and 0.289 μM, respectively), higher than that of doxorubicin (IC_{50} = 0.727 μM), whereas **4b**, **4c**, **5b** and **6a** displayed lower activity (IC_{50} = 1.44–5.01 μM). These results are correlated with the *in vitro* antimicrobial and antiproliferative screening results, suggesting that TOP IIβ could be the target for this class of compounds.

3. Computational studies

3.1. Molecular modeling

Structure-based drug design (SBDD) is a crucial step in the optimization process of potential drug candidates in drug discovery and pharmaceutical research [55,56]. SBDD tools enable accurate and efficient prediction of the preferential binding orientation of a lead compound to a three-dimensional protein structure or molecular target [55]. Molecular modeling is a valuable SBDD tool that is capable of identification of scaffolds and pharmacophoric units in the lead compounds that are directly involved in interactions with the molecular target [57–59]. Thus, a molecular modeling study based on the crystal structure of TOP IIβ in complex with DNA and etoposide (PDB code: 3QX3, https://www.rcsb.org/3d-view/3QX3/1) was performed in order to get an insight into the binding mode of the active compounds **5b, 7a** and **7b** to TOP IIβ. Binding mode of etoposide to the active site of TOP IIβ revealed two key interactions; π-π stacking with Arg503 residue and hydrogen bonding with Asp479 residue. Results of the docking studies evidenced that all of the investigated compounds displayed hydrogen bonding interaction with Asp479 residue in the active

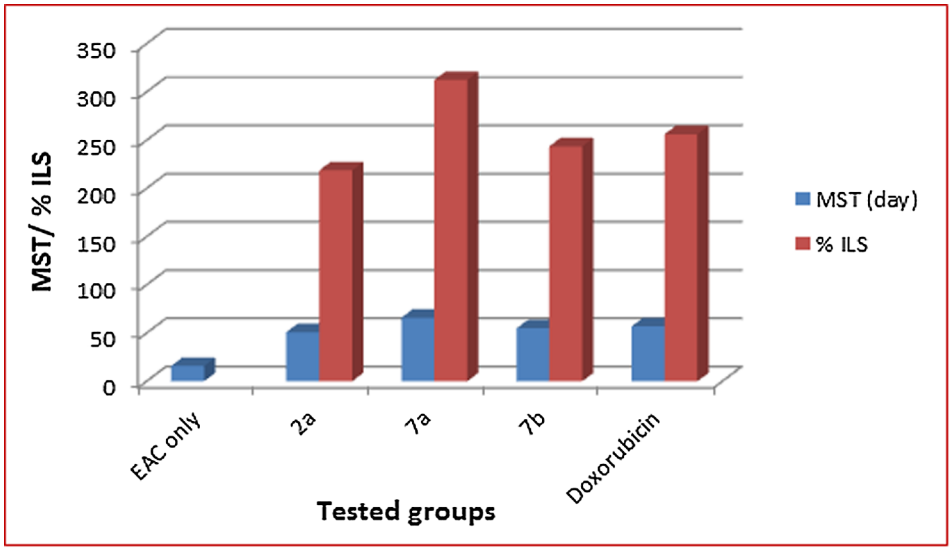

Fig. 4. Influence of **2a**, **7a** and **7b** on MST and % ILS of mice carrying EAC.

Table 5
Influence of **2a**, **7a** and **7b** on tumor parameters in mice carrying EAC.

Group	Viable tumor cell count (10^6/mL)[a]	Tumor volume (mL)[a]
Normal	na	na
EAC only	72.76	9.60
2a	30.34	1.92
7a	**18.50**	**1.05**
7b	**22.65**	**1.23**
Doxorubicin	15.25	2.00

[a] Results are the mean of three readings.
na: not assigned.
Bold values shed light on the preferable results.

Table 6
Influence of **2a**, **7a** and **7b** on hematological parameters of mice carrying EAC.

Group	Hb (g/dl)[a]	RBCs (10^6/mm^3)[a]	WBCs (10^3/mm^3)[a]
Normal	13.16	6.14	5.49
EAC only	7.86	3.57	20.25
2a	11.99	5.18	9.15
7a	**12.94**	**6.15**	**8.31**
7b	**12.52**	**5.86**	**8.47**
Doxorubicin	12.25	5.56	8.79

[a] Results are the mean of three readings.
Bold values shed light on the preferable results.

site of TOP IIβ. However, only compounds **7a** and **7b** featured additional hydrogen bonding formation with Arg503 residue which is consistent with their improved TOP IIβ inhibitory activity in comparison to the other investigated compounds (Table 9). These results revealed that presence of two hydrogen bond donors in close proximity to one hydrogen bond acceptor in the small molecule is crucial for optimum hydrogen bonding interactions with Asp479 and Arg503, the key residues in the target binding site. These findings should facilitate future development of potent TOP IIβ inhibitors based on the lead compounds identified in this study.

Moreover, compounds **7a** and **7b** displayed favorable binding to TOP IIβ with estimated binding energy of −22.7 and −23.4 kcal/mol, respectively, in comparison to doxorubicin and etoposide that possessed binding energy of −20.6 and −21.9 kcal/mol, respectively (Table 10). Compounds **7a** and **7b** featured comparable orientation in the active site of TOP IIβ, however, **7b** displayed additional hydrophobic interaction with Tyr821 and Arg820 residues which accounts for its favorable binding to the target receptor as well as more potent inhibition of TOP IIβ activity. The 3D interactions of **7a** and **7b** with the active site of TOP IIβ were created by Molegro 2.5 software [60] and depicted in Figs. 7A and 8A, respectively. The detailed analyses of

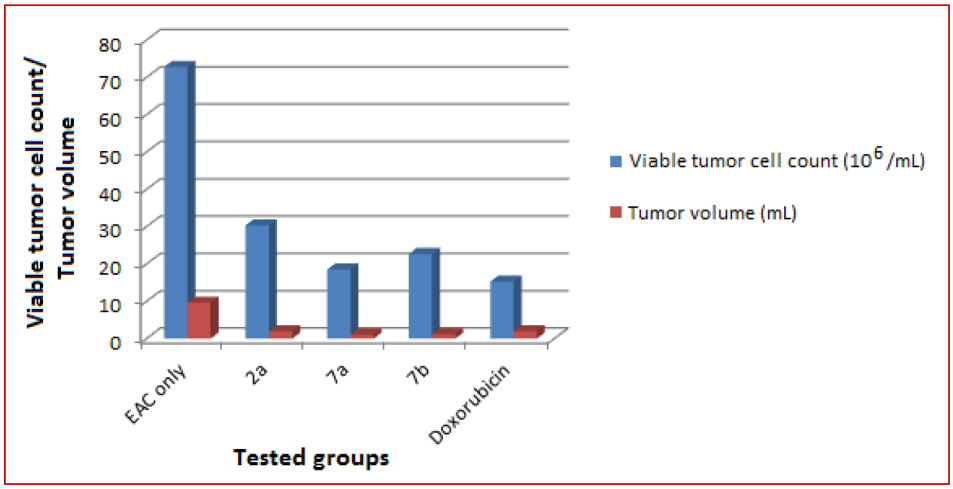

Fig. 5. Influence of **2a**, **7a** and **7b** on tumor parameters in mice carrying EAC.

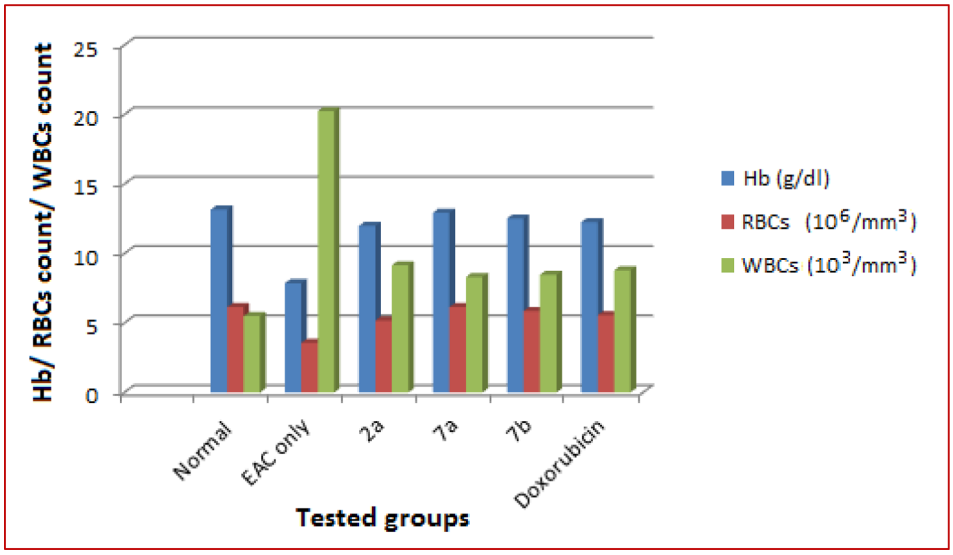

Fig. 6. Influence of **2a**, **7a** and **7b** on hematological parameters of mice carrying EAC.

Table 7
Results of cytotoxicity against normal cells.

Comp. No.	IC_{50} (μM)[a,b]	
	WI38	WISH
2a	23.71 ± 1.5	11.81 ± 1.1
7a	58.57 ± 3.8	63.41 ± 3.7
7b	41.23 ± 2.3	25.63 ± 1.6
Doxorubicin	6.68 ± 0.5	8.14 ± 0.9

[a] IC_{50} values = mean ± SD of three readings.
[b] IC_{50} (μM): strong (1–20); moderate (21–50); weak (51–100); non-cytotoxic (> 100).

Table 8
DNA-binding affinity of **2a, 4a-c, 5b, 6a** and **7a,b**.

Comp. No.	Methyl green/DNA (IC_{50}, μM)[a]
2a	42.39 ± 2.7
4a	43.35 ± 2.9
4b	82.38 ± 4.2
4c	59.03 ± 3.3
5b	**27.16 ± 1.6**
6a	63.47 ± 3.5
7a	**35.12 ± 2.3**
7b	**36.20 ± 2.4**
Doxorubicin	31.27 ± 1.8

[a] IC_{50} values = mean ± SD of three readings.
Bold values shed light on the preferable results.

Table 9
TOP IIβ inhibitory effect of **2a, 4a-c, 5b, 6a** and **7a,b**.

Comp. No.	IC_{50} (μM)[a]
2a	**0.355**
4a	**0.433**
4b	1.55
4c	1.44
5b	5.01
6a	1.53
7a	**0.314**
7b	**0.289**
Doxorubicin	0.727

[a] IC_{50} values = mean of three readings.
Bold values shed light on the preferable results.

Table 10
Binding energy of **5b, 7a** and **7b**.

Comp. No.	Binding energy (kcal/mol)
5b	−20.5
7a	**−22.7**
7b	**−23.4**
Doxorubicin	−20.6
Etoposide	−21.9

Bold values shed light on the preferable results.

binding interactions of **7a** and **7b** to TOP IIβ were created by Lead IT 2.3.2 software [61] and displayed in their 2D binding mode featuring key hydrogen bonding interactions with Asp479 and Arg503 residues (Figs. 7B and 8B, respectively) similarly to etoposide and doxorubicin (Fig. 9A and B, respectively). Taking into advisement the analysis of docking results and *in vitro* enzyme assay, it is proved that **7a** and **7b** are the most active analogs in this study as TOP IIβ inhibitors. These results agreed with *in vitro* antiproliferative screening which demonstrated that **7a** and **7b** are the most efficacious members in this study against HepG2 and HCT-116 cell lines (Table 3). 3D and 2D pharmacophores for the structures of **7a** and **7b** were built by LigandScout 4.1 software [62] (Fig. 10A and B) and (Fig. 11A and B), respectively. The overlay of the pharmacophore of **7a** and **7b** to the pharmacophore of binding of etoposide to TOP IIβ are depicted in Figs. 10C and 11C, respectively. The inspected pharmacophoric features of **7b** include hydrogen bond donors and acceptors as directed vectors, positive and negative ionizable regions as well as lipophilic areas that are illustrated by spheres. The pharmacophores of **7a** and **7b** would enable the design of new more potent TOP IIβ inhibitors as prospective antimicrobial and antitumor agents.

3.2. *In silico simulation studies*

In silico studies are performed *via* computer simulation, and they have the potential to accelerate the rate of drug discovery. They are very crucial in the expectation of physicochemical properties, pharmacokinetics and toxicity of compounds [63]. Thus, the new compounds were analyzed for the expectancy of Lipinski's rule [64] and Veber's criteria [65] applying Molinspiration software [66]. Likewise, carcinogenicity [67], solubility and drug score values [68] of the new members were prophesied.

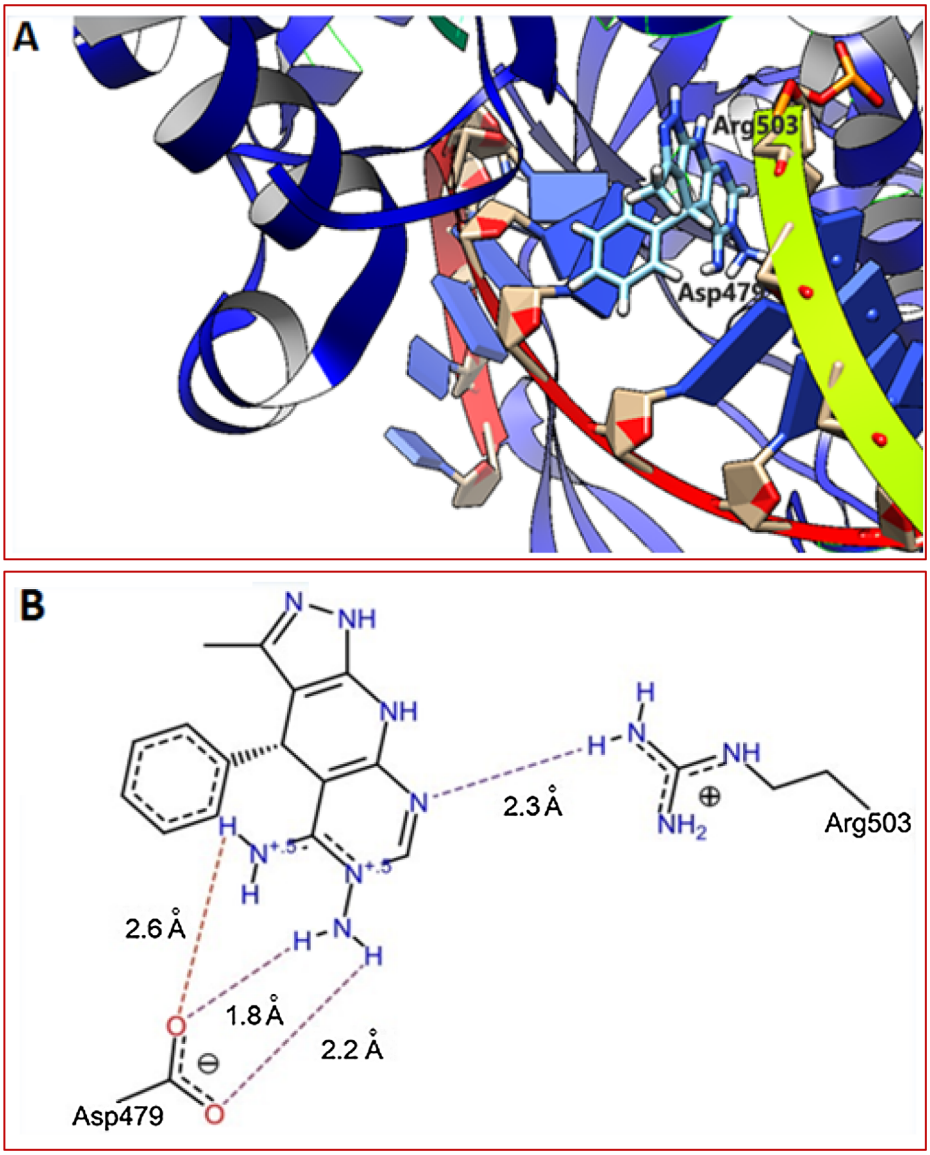

Fig. 7. (A) 3D Interaction of **7a** with the active site of TOP IIβ. The following refers to color of atoms: cyan for carbon, white for hydrogen and blue for nitrogen. **(B)** 2D Interaction of **7a** with the active site of TOP IIβ. Hydrogen bonds are represented by dashed lines.

3.2.1. Molinspiration calculations

Lipinski's rule is beneficial in the prediction of oral absorption of drugs [64], and it is based on the physicochemical properties of the investigated compounds. Also, topological polar surface area (TPSA) and number of rotatable bonds (Nrotb) influence drug absorption [65].

Molinspiration software [66] was applied for analyses of TPSA, Nrotb and the parameters of Lipinski's rule of the new derivatives. Results (Supplementary Table S1) indicated that all of the analyzed compounds (except **9a-c)** are under the acceptable norms of Lipinski's rule, TPSA and Nrotb.

3.2.2. Prediction of carcinogenicity

PreADMET software [67] was applied to predict the potential carcinogenic effect in mice and rats. Data presented in Supplementary Table S2 manifested that the new members (except **7a-c** and **9c**) are foreseen to have no carcinogenic effect in mice. Further, they are predicted to have no carcinogenic effect in rats (except **2c, 4c, 7a, 7c** and **8c**).

3.2.3. Solubility and drug score calculations

The aqueous solubility of a compound crucially affects its absorption and distribution properties. Typically, low solubility goes along with bad absorption; therefore, the main goal is to avoid poorly soluble compounds. It is well known that more than 80% of drugs in the market have predestined solubility values above −4. As shown in Supplementary Table S2, compounds **2a, 2c, 4a, 4c, 5a, 5c, 6a-c, 7a** and **7c** have solubility values above −4, and they are anticipated to exhibit good absorption and distribution properties.

The drug score combines cLogP, solubility, molecular weight, drug-likeness and toxicity risks in one handy value that could be applied to judge the compound's overall potential to qualify for a drug [69]. A drug score value of 0.5 or more makes the compound a promising lead for future development of safe and efficient drugs [69]. The drug score values of the new analogs were calculated and compared to that of ciprofloxacin, ampicillin, fluconazole and doxorubicin using Molsoft software [68]. All of the analyzed analogs have good drug score values (Supplementary Table S2).

4. Conclusion

Antimicrobial assay results confirmed that **4a** has moderate to good and broad-spectrum antimicrobial activity over all tested microbes, and

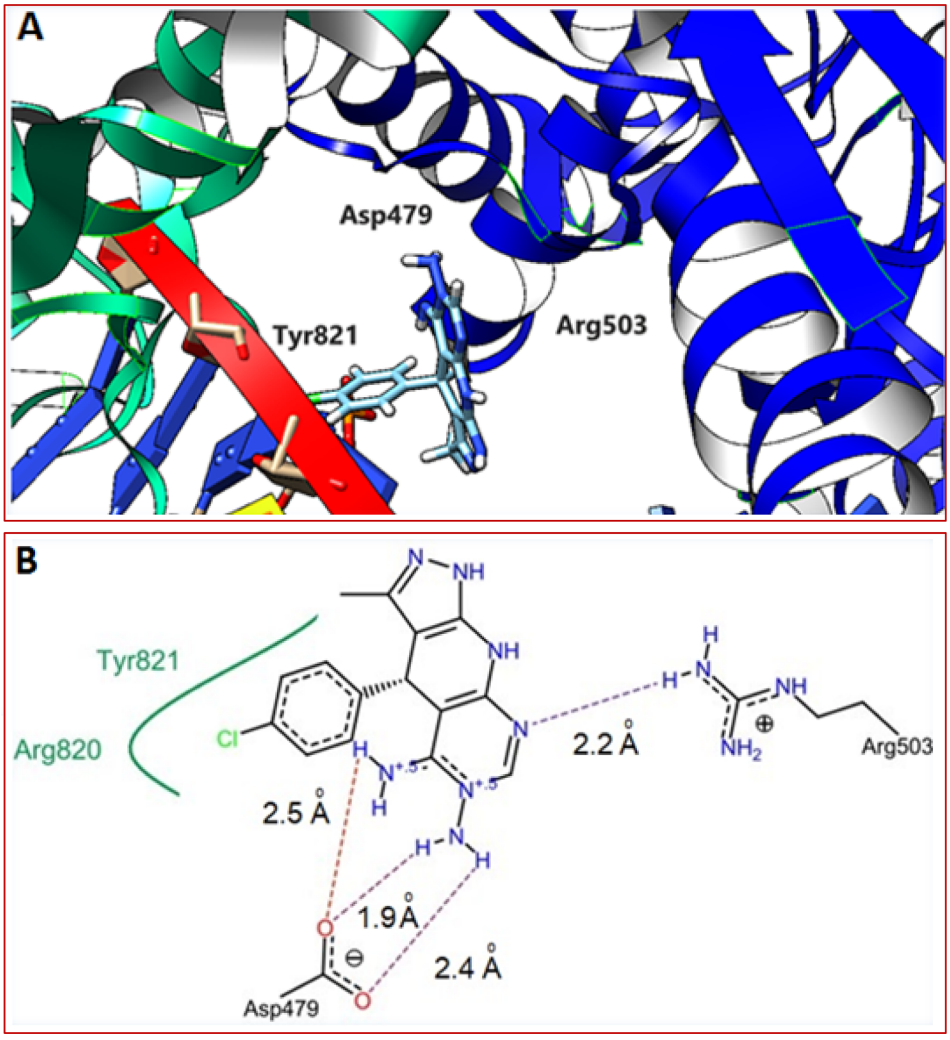

Fig. 8. (A) 3D Interaction of **7b** with the active site of TOP IIβ. The following refers to color of atoms: cyan for carbon, white for hydrogen, blue for nitrogen and green for chlorine. **(B)** 2D Interaction of **7b** with the active site of TOP IIβ. Hydrogen bonds are represented by dashed lines. Hydrophobic interactions are represented by green solid lines.

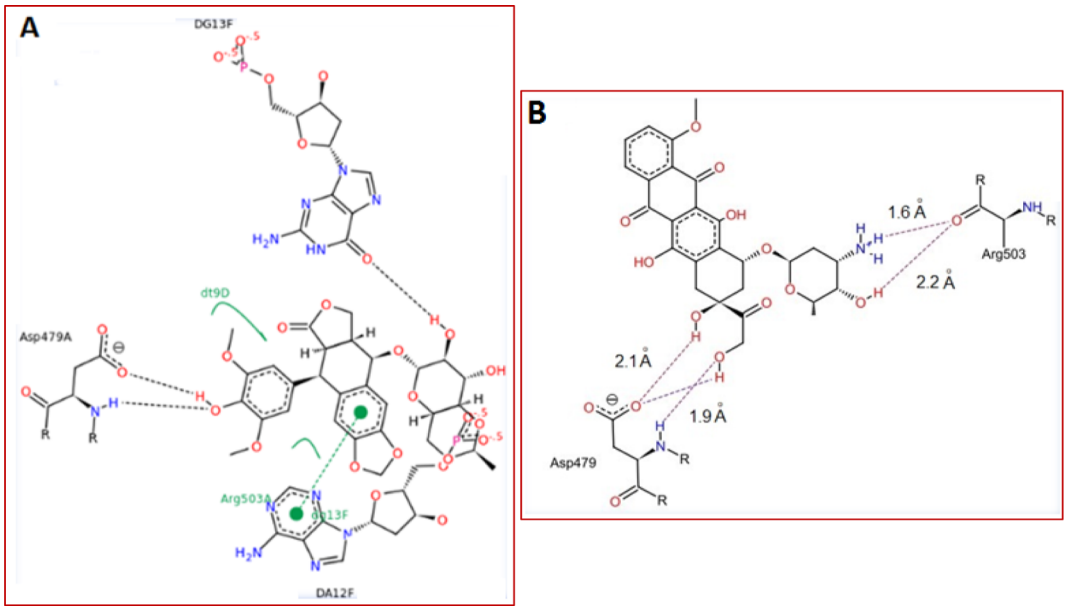

Fig. 9. (A) 2D Interaction of etoposide with the active site of TOP IIβ. **(B)** 2D Interaction of doxorubicin with the active site of TOP IIβ. Hydrogen bonds are represented by dashed lines. Hydrophobic interactions are represented by green solid lines.

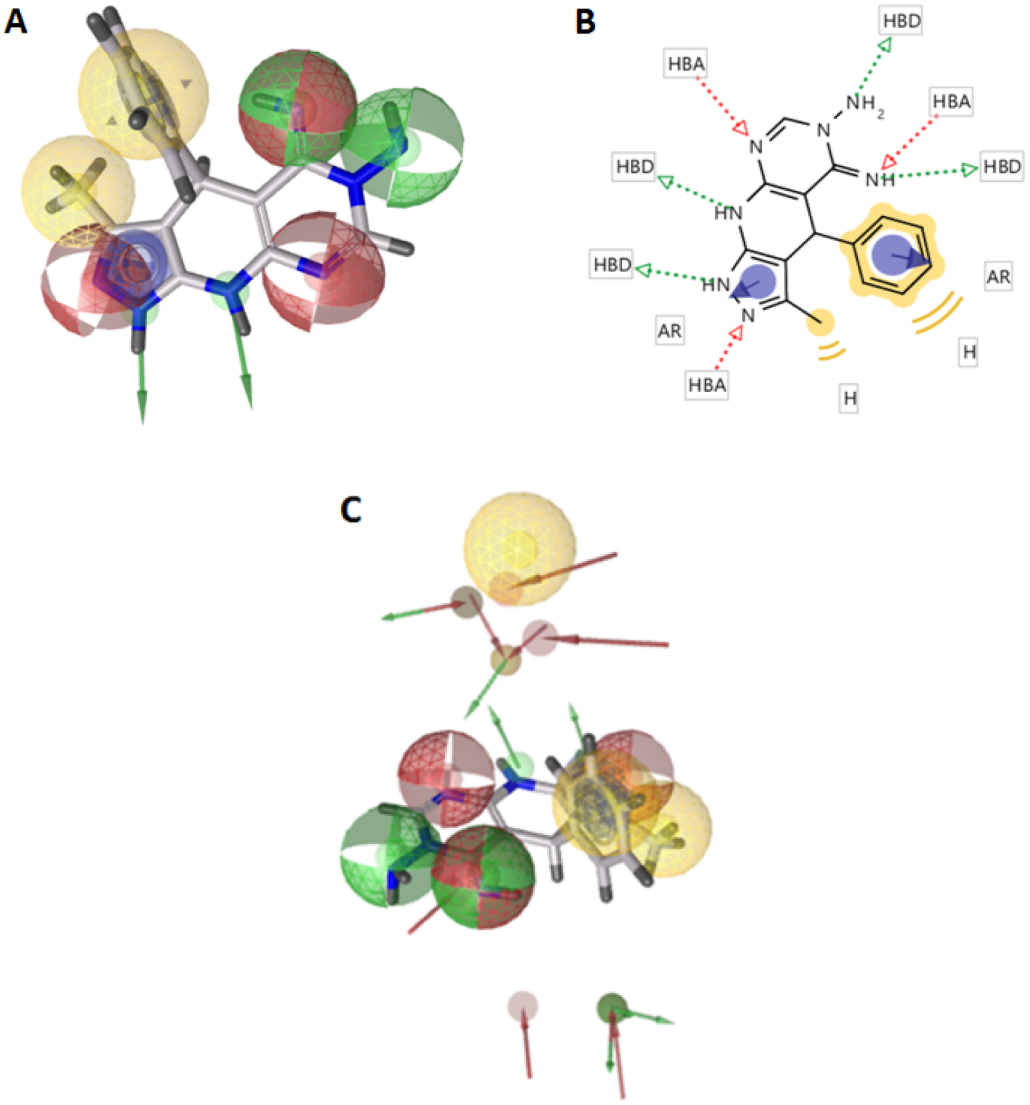

Fig. 10. (A) 3D Pharmacophore of **7a**; pharmacophore color code is yellow for hydrophobic regions, red for hydrogen acceptors and green for hydrogen donors. **(B)** 2D Pharmacophore of **7a**; HBA is hydrogen bond acceptor, HBD is hydrogen bond donor, AR is aryl and H is hydrophobic center. **(C)** The overlay of the pharmacophore of **7a** to the pharmacophore of binding of etoposide to TOP IIβ.

strong QS inhibitory effect. Compounds **4b** and **4c** displayed considerable activity on the chosen Gram-positive bacteria and *A. fumigatus*, whereas **6a** exhibited acceptable activity on *B. cereus* and *P. aeruginosa*, and strong QS inhibitory effect. Also, **7a** and **7b** showed good activity over the tested Gram-negative bacteria and fungi, and moderate activity over the tested Gram-positive bacteria, as well as strong QS inhibitory effect. Shifting to *in vitro* antiproliferative assay results, **7a** exhibited potent antiproliferative efficacy toward all tested cell lines; moreover, **2a** and **7b** showed promising efficacy on the three cell lines. Additionally, **7a** and **7b** displayed eminent *in vivo* antitumor activity against EAC cells. Furthermore, the two compounds showed lower cytotoxicity than doxorubicin on WI38 and WISH normal cells; therefore, they might be used as effective and selective antitumor agents. Results of DNA-binding testing illustrated that **2a, 5b** and **7a** have strong affinity; thus, they are prophesied to act through binding to DNA. Results of TOP IIβ inhibitory activity affirmed that **2a, 4a, 7a** and **7b** have strong TOP IIβ inhibitory activity, higher than that of doxorubicin. Thus, the active compounds in the current research are forecasted to display their biological activity through binding to DNA and/or targeting TOP IIβ. Furthermore, docking results boosted the efficacious binding interactions of **7a** and **7b** with TOP IIβ. *In silico* results clarified that most of the inspected compounds are in harmony with Veber's and Lipinski's rule parameters, and they are foreseen to show good oral absorption. The obtained data assured that rational design of the new fused pyrazolopyridines with predicted antimicrobial and antitumor activities was satisfactory; consequently, the active derivatives in this study will be exposed to additional structural alterations hoping to attain new more potent derivatives.

5. Experimental

Stuart melting point apparatus (SMP30) was employed to determine melting points °C. Unicam SP 1000 IR spectrometer (ν in cm^{-1}) was utilized to record IR spectra (KBr disc). ^{1}H and ^{13}C NMR spectra were obtained on Brucker 500 MHz spectrometer in DMSO-d_6. JEOL JMS-600H spectrometer (70 eV) was used for recording mass spectra. Microanalyses (% C, H, N) were achieved, and they were in concord with the suggested structures. TLC plates (silica gel 60 F254) were employed for regulating the advance of reactions, and UV was used to visualize the spots. Elution was performed by chloroform/methanol (9:1). *Ortho* aminonitriles **1a-c** were synthesized following the former method [28]. 2-Hydroxybenzohydrazide and 2-(2-phenyl-1*H*-benzimidazol-1-yl)acetohydrazide were prepared adopting the literature methods [70] and [71], respectively.

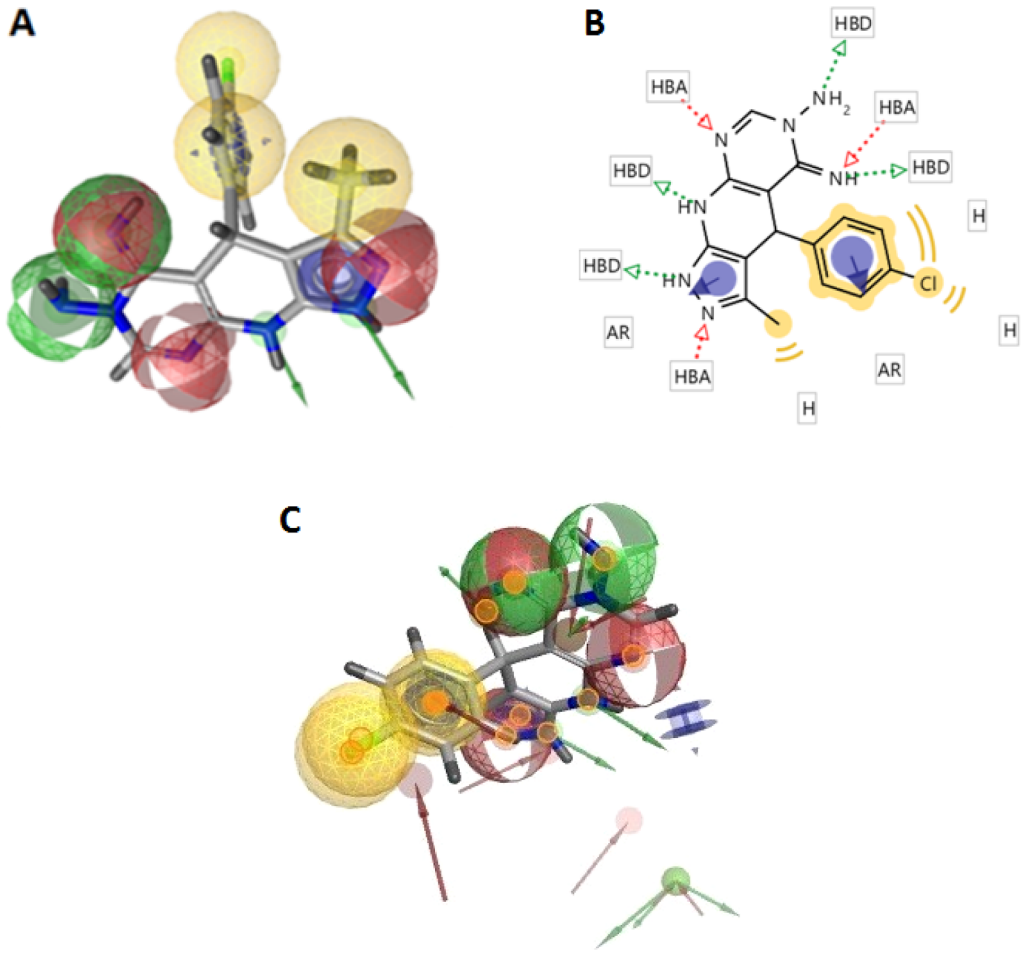

Fig. 11. (A) 3D Pharmacophore of **7b**; pharmacophore color code is yellow for hydrophobic regions, red for hydrogen acceptors and green for hydrogen donors. **(B)** 2D Pharmacophore of **7b**; HBA is hydrogen bond acceptor, HBD is hydrogen bond donor, AR is aryl and H is hydrophobic center. **(C)** The overlay of the pharmacophore of **7b** to the pharmacophore of binding of etoposide to TOP IIβ.

5.1. Chemistry

5.1.1. Synthesis of compounds 2a-c

A solution of **1a-c** (0.002 mol) and concentrated HCl (2 mL) in glacial acetic acid (10 mL) was refluxed for 16–20 h. The mixture was poured onto ice and neutralized with 1 *N* NaOH solution. The precipitated solid was filtered and crystallized from ethanol.

5.1.1.1. 3,7-Dimethyl-4-phenyl-1,4,6,9-tetrahydro-5H-pyrazolo[4′,3′:5,6] pyrido[2,3-d]pyrimidin-5-one ***(2a)***. Yield 76%, m.p. 200–202 °C. IR: 3404, 3284 (3NH), 1690 (C=O). ^{1}H NMR *δ*: 1.89 (s, 3H, CH_3), 2.06 (s, 3H, CH_3), 4.14 (s, 1H, C_4-H), 7.09–7.31 (m, 5H, Ar-H), 8.93 (s, 1H, NH), 10.85 (s, 2H, 2NH). ^{13}C NMR *δ*: 10.2, 25.7, 36.2, 102.2, 102.9, 125.8, 127.3, 127.4, 127.9, 128.1, 136.4, 145.0, 159.3, 173.3. MS *m/z* (%): 295 (35, $M^+ + 2$), 294 (28, $M^+ + 1$), 275 (100.00). Anal. Calcd (Found) for $C_{16}H_{15}N_5O$ (293.33): C, 65.52 (65.74); H, 5.15 (5.36); N, 23.88 (24.14) %.

5.1.1.2. 4-(4-Chlorophenyl)-3,7-dimethyl-1,4,6,9-tetrahydro-5H-pyrazolo [4′,3′:5,6]pyrido[2,3-d]pyrimidin-5-one ***(2b)***. Yield 70%, m.p. 177–179 °C (decomp.). IR: 3420 (3NH), 1682 (C=O). ^{1}H NMR *δ*: 1.89 (s, 3H, CH_3), 2.18 (s, 3H, CH_3), 4.56 (s, 1H, C_4-H), 7.21–7.89 (m, 4H, Ar-H), 9.99 (s, 1H, NH), 11.32 (s, 1H, NH), 11.49 (s, 1H, NH). ^{13}C NMR *δ*: 10.4, 21.4, 31.9, 103.2, 104.5, 127.8, 129.4, 130.0, 133.9, 140.8, 160.7, 165.4, 166.8, 172.0. MS *m/z* (%): 330 (2.18, $M^+ + 2$), 329 (1.98, $M^+ + 1$), 328 (6.75, M^+), 109 (100.00). Anal. Calcd (Found) for $C_{16}H_{14}ClN_5O$ (327.77): C, 58.63 (58.86); H, 4.31 (4.11); N, 21.37 (21.71) %.

5.1.1.3. 4-(4-(Dimethylamino)phenyl)-3,7-dimethyl-1,4,6,9-tetrahydro-5H-pyrazolo[4′,3′:5,6]pyrido[2,3-d]pyrimidin-5-one ***(2c)***. Yield 67%, m.p. 150–152 °C. IR: 3423, 3384 (3NH), 1687 (C=O). ^{1}H NMR *δ*: 1.89 (s, 3H, CH_3), 2.03 (s, 3H, CH_3), 2.80 (s, 6H, $N(CH_3)_2$), 4.31 (s, 1H, C_4-H), 6.41 (d, 2H, *J* = 8.0 Hz, Ar-H), 6.97 (d, 2H, *J* = 8.5 Hz, Ar-H), 7.01 (s, 1H, NH), 7.83 (s, 1H, NH), 7.96 (s, 1H, NH). ^{13}C NMR *δ*: 10.5, 22.5, 32.4, 42.3, 100.7, 112.6, 112.7, 127.8, 128.5, 135.0, 148.6, 148.7, 148.8, 149.2, 172.1. MS *m/z* (%): 336 (12.75, M^+), 253 (100.00). Anal. Calcd (Found) for $C_{18}H_{20}N_6O$ (336.40): C, 64.27 (63.89); H, 5.99 (5.71); N, 24.98 (24.61) %.

5.1.2. Synthesis of 7-chloromethyl-4-(4-(dimethylamino)phenyl)-3-methyl-1,4,6,9-tetrahydro-5H-pyrazolo[4′,3′:5,6]pyrido[2,3-d]pyrimidin-5-one ***(3c)***

A mixture of **1c** (0.589 g, 0.002 mol) and chloroacetyl chloride (0.226 g, 0.002 mol) in DMF (5 mL) was refluxed for 10 h. The mixture was poured onto ice, and precipitate attained was filtered and crystallized from dioxane.

Yield 70%, m.p. 170–171 °C. IR: 3421, 3372, 3220 (3NH), 1667 (C=O). ^{1}H NMR *δ*: 1.71 (s, 3H, CH_3), 2.87 (s, 6H, $N(CH_3)_2$), 3.89 (s, 2H, CH_2), 4.35 (s, 1H, C_4-H), 6.65 (d, 2H, *J* = 7.5 Hz, Ar-H), 7.21 (d, 2H, *J* = 7.5 Hz, Ar-H), 7.75 (s, 1H, NH), 8.28 (s, 1H, NH), 9.26 (s, 1H, NH). ^{13}C NMR *δ*: 10.2, 35.8, 41.3, 59.5, 111.3, 111.6, 112.2, 128.8, 129.6, 131.5, 145.3, 161.7, 162.0, 162.3, 174.2. MS *m/z* (%): 372 (21.65, $M^+ + 1$), 371 (14.37, M^+), 57 (100.00). Anal. Calcd (Found) for

$C_{18}H_{19}ClN_6O$ (370.84): C, 58.30 (58.63); H, 5.16 (4.91); N, 22.66 (22.37) %.

5.1.3. Synthesis of analogs ***4a-c***

Compounds **4a-c** were synthesized applying a similarly reported method [36].

5.1.3.1. 6-Methyl-5-phenyl-3,5,8,9-tetrahydro-4H-pyrazolo[4′,3′:5,6] pyrido[2,3-d][1,2,3]triazin-4-one ***(4a)***. Yield 71%, m.p. 135–136 °C, (dioxane/water (2:1)). IR: 3450 (3NH), 1693 (C=O). ^{1}H NMR *δ*: 2.07 (s, 3H, CH_3), 4.00 (s, 1H, C_5-H), 7.57–7.59 (m, 5H, Ar-H), 8.03 (s, 2H, 2NH), 8.34 (s, 1H, NH). ^{13}C NMR *δ*: 11.6, 36.1, 103.8, 115.2, 127.8, 128.8, 129.3, 133.1, 140.4, 154.5, 155.5, 163.3. MS *m/z* (%): 282 (0.28, $M^+ + 2$), 281 (0.34, $M^+ + 1$), 280 (0.30, M^+), 51 (100.00). Anal. Calcd (Found) for $C_{14}H_{12}N_6O$ (280.29): C, 59.99 (59.63); H, 4.32 (4.61); N, 29.98 (29.74) %.

5.1.3.2. 5-(4-Chlorophenyl)-6-methyl-3,5,8,9-tetrahydro-4H-pyrazolo [4′,3′:5,6]pyrido[2,3-d][1,2,3]triazin-4-one ***(4b)***. Yield 75%, m.p. 198–199 °C, (dioxane/water (2:1)). IR: 3440 (3NH), 1686 (C=O). ^{1}H NMR *δ*: 2.41 (s, 3H, CH_3), 4.42 (s, 1H, C_5-H), 7.25 (s, 1H, NH), 7.50 (d, 2H, *J* = 8.5 Hz, Ar-H), 7.66 (s, 1H, NH), 7.93 (d, 2H, *J* = 8.5 Hz, Ar-H), 9.99 (s, 1H, NH). ^{13}C NMR *δ*: 12.7, 34.8, 105.0, 117.8, 128.3, 131.1, 134.8, 137.8, 139.4, 141.5, 155.5, 166.5. MS *m/z* (%): 317 (0.3, $M^+ + 2$), 315 (0.86, M^+), 57 (100.00). Anal. Calcd (Found) for $C_{14}H_{11}ClN_6O$ (314.73): C, 53.43 (53.14); H, 3.52 (3.81); N, 26.70 (26.46) %.

5.1.3.3. 5-(4-(Dimethylamino)phenyl)-6-methyl-3,5,8,9-tetrahydro-4H-pyrazolo[4′,3′:5,6]pyrido[2,3-d][1,2,3]triazin-4-one ***(4c)***. Yield 60%, m.p. 120–121 °C, (dioxane/water (2:1)). IR: 3371 (3NH), 1683 (C=O). ^{1}H NMR *δ*: 2.07 (s, 3H, CH_3), 3.03 (s, 6H, $N(CH_3)_2$), 4.47 (s, 1H, C_5-H), 7.12 (d, 2H, *J* = 8.5 Hz, Ar-H), 7.93 (d, 2H, *J* = 8.0 Hz, Ar-H), 8.61 (s, 2H, 2NH), 8.72 (s, 1H, NH). ^{13}C NMR *δ*: 10.6, 30.1, 42.2, 114.2, 115.2, 118.2, 130.6, 131.2, 133.9, 148.4, 148.9, 158.4, 169.9. MS *m/z* (%): 325 (0.16, $M^+ + 2$), 324 (0.02, $M^+ + 1$), 323 (0.08, M^+), 57 (100.00). Anal. Calcd (Found) for $C_{16}H_{17}N_7O$ (323.36): C, 59.43 (59.78); H, 5.30 (4.98); N, 30.32 (30.61) %.

5.1.4. Synthesis of ethyl formimidates ***5a-c***

A mixture of **1a–c** (0.01 mol) and triethyl orthoformate (10 mL) was refluxed for 10–12 h. Excess reagent was evaporated, and the residue remained was triturated with ice, filtered and crystallized from ethanol.

5.1.4.1. Ethyl N-(5-cyano-3-methyl-4-phenyl-4,7-dihydro-1H-pyrazolo [3,4-b]pyridin-6-yl)formimidate ***(5a)***. Yield 75%, m.p. 130–132 °C. IR: 3312 (2NH), 2205 (C≡N). ^{1}H NMR *δ*: 1.29 (t, 3H, *J* = 7.5 Hz, $OCH_2C\underline{H_3}$), 1.79 (s, 3H, CH_3), 4.26–4.30 (q, 2H, *J* = 7.0 Hz, $OC\underline{H_2}CH_3$), 4.58 (s, 1H, C_4-H), 7.15–7.36 (m, 5H, Ar-H), 8.57 (s, 1H, CH = N), 12.27 (s, 1H, NH), 12.35 (s, 1H, NH). ^{13}C NMR *δ*: 9.7, 13.9, 36.2, 63.9, 81.0, 96.9, 118.1, 127.9, 128.5, 128.7, 135.9, 136.1, 154.2, 158.4, 161.3. MS *m/z* (%): 309 (7.35, $M^+ + 2$), 308 (24.99, $M^+ + 1$), 307 (2.51, M^+), 77 (100.00). Anal. Calcd (Found) for $C_{17}H_{17}N_5O$ (307.36): C, 66.43 (66.15); H, 5.58 (5.91); N, 22.79 (22.58) %.

5.1.4.2. Ethyl N-(4-(4-chlorophenyl)-5-cyano-3-methyl-4,7-dihydro-1H-pyrazolo[3,4-b]pyridin-6-yl)formimidate ***(5b)***. Yield 70%, m.p. 153–154 °C. IR: 3331, 3215 (2NH), 2214 (C≡N). ^{1}H NMR *δ*: 1.30 (t, 3H, *J* = 6.5 Hz, $OCH_2C\underline{H_3}$), 1.98 (s, 3H, CH_3), 4.25–4.29 (q, 2H, *J* = 7.0 Hz, $OC\underline{H_2}CH_3$), 4.35 (s, 1H, C_4-H), 7.35 (d, 2H, *J* = 8.0 Hz, Ar-H), 7.59 (d, 2H, *J* = 8.0 Hz, Ar-H), 7.95 (s, 1H, CH=N), 10.99 (s, 1H, NH), 11.41 (s, 1H, NH). ^{13}C NMR *δ*: 10.1, 14.7, 35.4, 61.1, 79.7, 91.7, 116.4, 128.9, 129.1, 130.5, 132.6, 138.1, 155.1, 159.5, 162.9. MS *m/z* (%): 344 (3.72, $M^+ + 2$), 342 (10.99, M^+), 74 (100.00). Anal. Calcd (Found) for $C_{17}H_{16}ClN_5O$ (341.80): C, 59.74 (60.11); H, 4.72 (4.51); N, 20.49 (20.73) %.

5.1.4.3. Ethyl N-(5-cyano-4-(4-(dimethylamino)phenyl)-3-methyl-4,7-dihydro-1H-pyrazolo[3,4-b]pyridin-6-yl)formimidate ***(5c)***. Yield 71%, m.p. 126–128 °C. IR: 3328, 3209 (2NH), 2206 (C≡N). ^{1}H NMR *δ*: 1.26 (t, 3H, *J* = 7.5 Hz, $OCH_2C\underline{H_3}$), 1.80 (s, 3H, CH_3), 2.95 (s, 6H, N $(CH_3)_2$), 4.23–4.27 (q, 2H, *J* = 7.5 Hz, $OC\underline{H_2}CH_3$), 4.72 (s, 1H, C_4-H), 6.66 (d, 2H, *J* = 8.0 Hz, Ar-H), 7.07 (d, 2H, *J* = 8.0 Hz, Ar-H), 8.17 (s, 1H, CH = N), 10.92 (s, 1H, NH), 12.29 (s, 1H, NH). ^{13}C NMR *δ*: 9.8, 13.2, 36.6, 41.1, 61.9, 79.6, 97.4, 112.2, 117.1, 128.1, 129.6, 136.5, 149.6, 154.2, 163.5, 165.9. MS *m/z* (%): 351 (21.91, $M^+ + 1$), 350 (18.55, M^+), 157 (100.00). Anal. Calcd (Found) for $C_{19}H_{22}N_6O$ (350.43): C, 65.12 (65.47); H, 6.33 (6.12); N, 23.98 (23.68) %.

5.1.5. Synthesis of analogs ***6a-c***

A mixture of ethyl formimidate **5a-c** (0.002 mol) and ammonia 35% (5 mL) in ethanol (10 mL) was refluxed for 12–14 h. The solvent was evaporated and precipitate was triturated with ice, filtered and crystallized from dioxane.

5.1.5.1. 5-Amino-3-methyl-4-phenyl-4,9-dihydro-1H-pyrazolo[4′,3′:5,6] pyrido[2,3-d]pyrimidine ***(6a)***. Yield 71%, m.p. 140–141 °C. IR: 3372, 3311, 3169 (2NH, NH_2). ^{1}H NMR *δ*: 1.98 (s, 3H, CH_3), 4.65 (s, 1H, C_4-H), 6.85 (s, 2H, NH_2), 7.43–7.65 (m, 5H, Ar-H), 8.62 (s, 1H, Pyrimidine-H), 9.85 (s, 1H, NH), 10.43 (s, 1H, NH). ^{13}C NMR *δ*: 9.7, 42.1, 100.1, 112.7, 117.0, 127.9, 128.8, 128.9, 137.2, 144.3, 156.9, 159.9, 163.0. MS *m/z* (%): 279 (1.60, $M^+ + 1$), 278 (0.30, M^+), 69 (100.00). Anal. Calcd (Found) for $C_{15}H_{14}N_6$ (278.32): C, 64.73 (64.46); H, 5.07 (4.85); N, 30.20 (30.58) %.

5.1.5.2. 5-Amino-4-(4-chlorophenyl)-3-methyl-4,9-dihydro-1H-pyrazolo [4′,3′:5,6]pyrido[2,3-d]pyrimidine ***(6b)***. Yield 76%, m.p. 200–202 °C. IR: 3420 (2NH, NH_2). ^{1}H NMR *δ*: 2.02 (s, 3H, CH_3), 4.79 (s, 1H, C_4-H), 7.26 (s, 2H, NH_2), 7.58 (d, 2H, *J* = 8.5 Hz, Ar-H), 7.89 (d, 2H, *J* = 8.0 Hz, Ar-H), 8.71 (s, 1H, Pyrimidine-H), 10.13 (s, 1H, NH), 10.89 (s, 1H, NH). ^{13}C NMR *δ*: 10.3, 41.9, 97.5, 105.4, 129.4, 129.9, 130.0, 132.6, 136.0, 160.5, 162.5, 167.3, 169.6. MS *m/z* (%): 313 (1.25, M^+), 312 (0.30, $M^+ - 1$), 124 (100.00). Anal. Calcd for $C_{15}H_{13}ClN_6$ (312.76): C, 57.60 (57.86); H, 4.19 (4.41); N, 26.87 (27.16) %.

5.1.5.3. 5-Amino-4-(4-(dimethylamino)phenyl)-3-methyl-4,9-dihydro-1H-pyrazolo[4′,3′:5,6]pyrido[2,3-d]pyrimidine ***(6c)***. Yield 69%, m.p. 160–162 °C. IR: 3431 (2NH, NH_2). ^{1}H NMR *δ*: 2.08 (s, 3H, CH_3), 2.98 (s, 6H, $N(CH_3)_2$), 4.11 (s, 1H, C_4-H), 7.02 (d, 2H, *J* = 8.0 Hz, Ar-H), 7.47 (d, 2H, *J* = 8.0 Hz, Ar-H), 7.67 (s, 2H, NH_2), 8.71 (s, 1H, Pyrimidine-H), 10.12 (s, 1H, NH), 10.89 (s, 1H, NH). ^{13}C NMR *δ*: 9.9, 38.2, 41.3, 97.5, 103.6, 112.5, 127.8, 129.9, 135.9, 145.4, 160.5, 163.5, 166.8, 168.6. MS *m/z* (%): 323 (0.19, $M^+ + 2$), 322 (0.09, $M^+ + 1$), 321 (0.03, M^+), 69 (100.00). Anal. Calcd (Found) for $C_{17}H_{19}N_7$ (321.39): C, 63.53 (63.82); H, 5.96 (5.66); N, 30.51 (30.37) %.

5.1.6. Synthesis of analogs ***7a-c***

A mixture of **5a-c** (0.002 mol) and hydrazine hydrate 98% (1.0 g, 0.02 mol) in ethanol (10 mL) was refluxed for 8–10 h. The solution was cooled and the solid separated was filtered and crystallized from ethanol.

5.1.6.1. 6-Amino-5-imino-3-methyl-4-phenyl-1,4,5,9-tetrahydro-6H-pyrazolo[4′,3′:5,6]pyrido[2,3-d]pyrimidine ***(7a)***. Yield 80%, m.p. 115–116 °C. IR: 3434, 3367, 3213 (3NH, NH_2). ^{1}H NMR *δ*: 2.03 (s, 3H, CH_3), 3.05 (s, 2H, NH_2), 4.35 (s, 1H, C_4-H), 7.04–7.73 (m, 6H, Ar-H, Pyrimidine-H), 7.87 (s, 1H, NH), 8.71 (s, 1H, NH), 10.85 (s, 1H, NH). ^{13}C NMR *δ*: 12.2, 32.2, 101.8, 112.2, 127.1, 128.4, 128.9, 137.9, 148.2, 150.0, 159.5, 161.1, 161.6. MS *m/z* (%): 295 (1.69, $M^+ + 2$), 294 (2.12, $M^+ + 1$), 293 (3.06, M^+), 57 (100.00). Anal. Calcd (Found) for $C_{15}H_{15}N_7$ (293.33): C, 61.42 (61.11); H, 5.15 (4.87); N, 33.43 (33.65) %.

5.1.6.2. 6-Amino-4-(4-chlorophenyl)-5-imino-3-methyl-1,4,5,9-tetrahydro-6H-pyrazolo[4′,3′:5,6]pyrido[2,3-d]pyrimidine ***(7b)***. Yield 85%, m.p. 190–192 °C. IR: 3441, 3195 (3NH, NH_2). ^{1}H NMR δ: 1.82 (s, 3H, CH_3), 4.32 (s, 1H, C_4-H), 6.89 (s, 1H, NH), 7.35 (d, 2H, J = 7.5 Hz, Ar-H), 7.66 (d, 2H, J = 7.5 Hz, Ar-H), 7.82 (s, 1H, Pyrimidine-H), 8.05 (s, 1H, NH), 8.50 (s, 1H, NH), 8.96 (s, 2H, NH_2). ^{13}C NMR δ: 10.5, 31.8, 99.2, 112.2, 126.6, 131.5, 135.4, 136.6, 140.1, 142.6, 164.6, 168.7, 173.4. MS *m/z* (%): 328 (0.08, M^+), 69 (100.00). Anal. Calcd (Found) for $C_{15}H_{14}ClN_7$ (327.78): C, 54.97 (54.65); H, 4.31 (4.62); N, 29.91 (29.56) %.

5.1.6.3. 6-Amino-5-imino-4-(4-(dimethylamino)phenyl)-3-methyl-1,4,5,9-tetrahydro-6H-pyrazolo[4′,3′:5,6]pyrido[2,3-d]pyrimidine ***(7c)***. Yield 88%, m.p. 145–146 °C. IR: 3420, 3342, 3210 (3NH, NH_2). ^{1}H NMR δ: 2.18 (s, 3H, CH_3), 2.96 (s, 6H, $N(CH_3)_2$), 4.92 (s, 1H, C_4-H), 6.13 (s, 2H, NH_2), 6.75 (d, 2H, J = 9.0 Hz, Ar-H), 7.26 (d, 2H, J = 8.5 Hz, Ar-H), 7.79 (s, 1H, Pyrimidine-H), 9.36 (s, 1H, NH), 9.78 (s, 1H, NH), 11.34 (s, 1H, NH). ^{13}C NMR δ: 12.4, 29.3, 41.9, 106.3, 111.7, 112.1, 129.5, 129.7, 139.5, 143.5, 150.1, 151.9, 156.2, 159.8. MS *m/z* (%): 338 (0.18, $M^+ + 2$), 337 (0.19, $M^+ + 1$), 336 (0.19, M^+), 53 (100.00). Anal. Calcd (Found) for $C_{17}H_{20}N_8$ (336.40): C, 60.70 (60.43); H, 5.99 (6.21); N, 33.31 (33.12) %.

5.1.7. Synthesis of analogs ***8a,c*** *and* ***9a-c***

A mixture of **5a-c** (0.002 mol) and 2-hydroxybenzohydrazide (0.304 g, 0.002 mol) or 2-(2-phenyl-1*H*-benzimidazol-1-yl)acetohydrazide (0.533 g, 0.002 mol) in DMF (10 mL) was refluxed for 12–14 h. The solvent was evaporated and the remained solid was crystallized from dioxane to afford **8a,c** and **9a-c**, respectively.

5.1.7.1. 2-(2-Hydroxyphenyl)-10-methyl-11-phenyl-8,11-dihydro-7H-pyrazolo[4′,3′:5,6]pyrido[3,2-e][1,2,4]triazolo[1,5-c]pyrimidine ***(8a)***. Yield 70%, m.p. 125–126 °C. IR: 3483, 3425, 3368 (OH, 2NH). ^{1}H NMR δ: 1.91 (s, 3H, CH_3), 4.99 (s, 1H, C_{11}-H), 6.96–7.39 (m, 9H, Ar-H), 8.39 (s, 1H, Pyrimidine-H), 9.70 (s, 1H, OH), 11.02 (s, 1H, NH), 12.33 (s, 1H, NH). ^{13}C NMR δ: 9.7, 36.5, 102.7, 117.7, 117.8, 118.7, 119.8, 128.3, 128.7, 128.8, 129.7, 130.4, 136.4, 140.2, 144.0, 148.5, 152.3, 154.2, 158.5, 169.5. MS *m/z* (%): 396 (99.16, $M^+ + 1$), 395 (7.91, M^+), 319 (100.00). Anal. Calcd (Found) for $C_{22}H_{17}N_7O$ (395.43): C, 66.82 (66.61); H, 4.33 (4.65); N, 24.80 (25.15) %.

5.1.7.2. 2-(2-Hydroxyphenyl)-11-(4-(dimethylamino)phenyl)-10-methyl-8,11-dihydro-7H-pyrazolo[4′,3′:5,6]pyrido[3,2-e][1,2,4]triazolo[1,5-c]pyrimidine ***(8c)***. Yield 65%, m.p. 200–202 °C. IR: 3425 (OH, 2NH). ^{1}H NMR δ: 2.13 (s, 3H, CH_3), 3.04 (s, 6H, $N(CH_3)_2$), 4.34 (s, 1H, C_{11}-H), 6.61–6.85 (m, 2H, Ar-H), 7.19–7.66 (m, 7H, Ar-H, Pyrimidine-H), 8.25 (s, 1H, OH), 9.45 (s, 1H, NH), 9.65 (s, 1H, NH). ^{13}C NMR δ: 9.6, 39.6, 40.5, 103.1, 111.2, 111.3, 111.4, 111.5, 128.6, 130.8, 132.1, 132.9, 136.9, 137.0, 152.6, 154.2, 154.3, 161.6, 161.8, 168.9, 171.5. MS *m/z* (%): 440 (0.22, $M^+ + 2$), 439 (0.36, $M^+ + 1$), 438 (0.22, M^+), 57 (100.00). Anal. Calcd (Found) for $C_{24}H_{22}N_8O$ (438.50): C, 65.74 (65.43); H, 5.06 (4.78); N, 25.55 (25.23) %.

5.1.7.3. 10-Methyl-11-phenyl-2-((2-phenyl-1H-benzimidazol-1-yl)methyl)-8,11-dihydro-7H-pyrazolo[4′,3′:5,6]pyrido[3,2-e][1,2,4]triazolo[1,5-c]pyrimidine ***(9a)***. Yield 60%, m.p. 169–170 °C. ^{13}C NMR δ: 12.5, 42.0, 54.0, 110.0, 116.3, 118.5, 123.5, 123.8, 125.0, 127.8, 128.7, 130.0, 130.7, 131.9, 133.1, 133.9, 134.7, 135.9, 136.4, 141.9, 143.7, 145.4, 149.9, 157.8, 165.8, 179.7. Anal. Calcd (Found) for $C_{30}H_{23}N_9$ (509.58): C, 70.71 (70.34); H, 4.55 (4.93); N, 24.74 (24.37) %.

5.1.7.4. 11-(4-Chlorophenyl)-10-methyl-2-((2-phenyl-1H-benzimidazol-1-yl)methyl)-8,11-dihydro-7H-pyrazolo[4′,3′:5,6]pyrido[3,2-e][1,2,4]triazolo[1,5-c]pyrimidine ***(9b)***. Yield 75%, m.p. 200–202 °C. IR: 3425, 3368 (2NH). ^{1}H NMR δ: 1.98 (s, 3H, CH_3), 4.64 (s, 2H, CH_2), 5.22 (s, 1H, C_{11}-H), 7.10 (d, 2H, J = 7.5 Hz, Ar-H), 7.14–7.38 (m, 7H, Ar-H), 7.47–7.77 (m, 5H, Ar-H, Pyrimidine-H), 9.95 (s, 1H, NH), 10.55 (s, 1H, NH). ^{13}C NMR δ: 10.3, 40.6, 56.2, 111.1, 111.3, 119.6, 126.9, 127.1, 127.8, 128.1, 129.8, 129.9, 130.9, 131.3, 131.7, 131.8, 132.0, 132.9, 133.2, 139.7, 139.9, 143.9, 150.5, 154.1, 166.6, 169.9. MS *m/z* (%): 546 (5.48, $M^+ + 2$), 544 (15.60, M^+), 297 (100.00). Anal. Calcd (Found) for $C_{30}H_{22}ClN_9$ (544.02): C, 66.23 (66.54); H, 4.08 (3.89); N, 23.17 (23.51) %.

5.1.7.5. 11-(4-(Dimethylamino)phenyl)-10-methyl-2-((2-phenyl-1H-benzimidazol-1-yl)methyl)-8,11-dihydro-7H-pyrazolo[4′,3′:5,6]pyrido[3,2-e][1,2,4]triazolo[1,5-c]pyrimidine ***(9c)***. Yield 71%, m.p. 156–157 °C. IR: 3428 (2NH). ^{1}H NMR δ: 1.98 (s, 3H, CH_3), 2.86 (s, 6H, $N(CH_3)_2$), 4.85 (s, 2H, CH_2), 5.19 (s, 1H, C_{11}-H), 6.95–7.17 (m, 5H, Ar-H), 7.47–7.69 (m, 9H, Ar-H, Pyrimidine-H, 2NH), 8.16–8.17 (m, 2H, Ar-H). ^{13}C NMR δ: 10.5, 36.5, 41.2, 55.9, 102.9, 109.8, 113.0, 117.6, 118.2, 120.0, 124.9, 125.6, 125.8, 127.4, 128.0, 128.1, 129.9, 130.1, 136.6, 137.1, 137.2, 140.4, 145.4, 147.9, 159.1, 159.4, 169.2. MS *m/z* (%): 554 (0.2, $M^+ + 1$), 553 (0.72, M^+), 552 (1.66, $M^+ - 1$), 194 (100.00). Anal. Calcd (Found) for $C_{32}H_{28}N_{10}$ (552.65): C, 69.55 (69.19); H, 5.11 (4.88); N, 25.35 (25.17) %.

5.2. Biology

The procedures of biological evaluation are presented thoroughly in the supplementary file.

5.2.1. Antimicrobial and antiquorum-sensing testing

5.2.1.1. Antibacterial assay. Disc plate method and serial dilution method were applied for assessing the antibacterial activity [11,12,40]. The detailed procedures are presented in the supplementary file.

5.2.1.2. Antifungal assay. Disc plate method and serial dilution method were applied for assessing the antifungal activity [11,12,41,42]. The detailed procedures are presented in the supplementary file.

5.2.1.3. Antiquorum-sensing assay. Disc plate method was applied for assessing the anti-QS activity [11,12,43]. The detailed procedure is presented in the supplementary file.

5.2.2. Antitumor testing

5.2.2.1. In vitro antiproliferative assay. MTT assay method was applied for assessing the *in vitro* antiproliferative activity [46–48]. The detailed procedure is presented in the supplementary file.

5.2.2.2. In vivo antitumor assay. The previously reported procedure of *in vivo* antitumor testing was adopted [49–51], and presented in details in the supplementary file.

5.2.2.3. In vitro cytotoxicity assay. MTT assay method was applied for assessing the *in vitro* cytotoxicity [46–48]. The detailed procedure is presented in the supplementary file.

5.2.3. Mechanistic study

5.2.3.1. DNA-binding assay. Methyl green/DNA displacement assay was adopted for studying the DNA-binding affinity of the active compounds [53]. The detailed procedure is presented in the supplementary file.

5.2.3.2. Topoisomerase IIβ assay. Topoisomerase IIβ inhibition assay [54] was adopted for evaluating the TOP IIβ inhibitory activity of the active compounds. The detailed procedure is presented in the supplementary file.

Acknowledgements

Thanks to Holding Company for Biological Products and Vaccines (VACSERA), Egypt, for conducting antitumor, cytotoxicity and TOP IIβ assays.

Appendix A. Supplementary material

Supplementary data to this article can be found online at https://doi.org/10.1016/j.bioorg.2019.103109.

References

[1] F. Blanquart, S. Lehtinen, M. Lipsitch, C. Fraser, The evolution of antibiotic resistance in a structured host population, J. R. Soc. Interf. 15 (2018), https://doi.org/10.1098/rsif.2018.0040 20180040.
[2] J.O. Sekyere, J. Asante, Emerging mechanisms of antimicrobial resistance in bacteria and fungi: advances in the era of genomics, Future Microbiol. 13 (2018) 241–262.
[3] D.S. Haque, F. Ahmad, S.A. Dar, A. Jawed, R.K. Mandal, M. Wahid, M. Lohani, S. Khan, V. Singh, N. Akhter, Developments in strategies for quorum sensing virulence factor inhibition to combat bacterial drug resistance, Microb. Pathog. 121 (2018) 293–302.
[4] N.S. El-Gohary, M.T. Gabr, M.I. Shaaban, Synthesis, molecular modeling and biological evaluation of new pyrazolo[3,4-*b*]pyridine analogs as potential antimicrobial, antiquorum-sensing and anticancer agents, Bioorg. Chem. 89 (2019) 102976, https://doi.org/10.1016/j.bioorg.2019.102976.
[5] N.S. El-Gohary, M.I. Shaaban, Design, synthesis, antimicrobial, antiquorum-sensing and antitumor evaluation of new series of pyrazolopyridine derivatives, Eur. J. Med. Chem. 157 (2018) 729–742.
[6] N.S. El-Gohary, M.I. Shaaban, New pyrazolopyridine analogs: synthesis, antimicrobial, antiquorum-sensing and antitumor screening, Eur. J. Med. Chem. 152 (2018) 126–136.
[7] A.A. Abd Elhameed, N.S. El-Gohary, E.R. El-Bendary, M.I. Shaaban, S.M. Bayomi, Synthesis and biological screening of new thiazolo[4,5-*d*]pyrimidine and dithiazolo [3,2-*a*: 5′,4′-*e*]pyrimidinone derivatives as antimicrobial, antiquorum-sensing and antitumor agents, Bioorg. Chem. 81 (2018) 299–310.
[8] S.A. Abdel-Rahman, N.S. El-Gohary, E.R. El-Bendary, S.M. El-Ashry, M.I. Shaaban, Synthesis, antimicrobial, antiquorum-sensing, antitumor and cytotoxic activities of new series of cyclopenta(hepta)[*b*]thiophene and fused cyclohepta[*b*]thiophene analogs, Eur. J. Med. Chem. 140 (2017) 200–211.
[9] N.S. El-Gohary, M.I. Shaaban, Synthesis, antimicrobial, antiquorum-sensing and antitumor activities of new benzimidazole analogs, Eur. J. Med. Chem. 137 (2017) 439–449.
[10] N.S. El-Gohary, M.I. Shaaban, Synthesis and biological evaluation of a new series of benzimidazole derivatives as antimicrobial, antiquorum-sensing and antitumor agents, Eur. J. Med. Chem. 131 (2017) 255–262.
[11] N.S. El-Gohary, M.I. Shaaban, Antimicrobial and antiquorum-sensing studies. Part 3: synthesis and biological evaluation of new series of [1,3,4]thiadiazole and fused [1,3,4]thiadiazole derivatives, Arch. Pharm. Chem. Life Sci. 348 (2015) 283–297.
[12] N.S. El-Gohary, M.I. Shaaban, Synthesis, antimicrobial, antiquorum-sensing, and cytotoxic activities of new series of isoindoline-1,3-dione, pyrazolo[5,1-*a*]isoindole and pyridine derivatives, Arch. Pharm. Chem. Life Sci. 348 (2015) 666–680.
[13] R.A. Al-Haidari, M.I. Shaaban, S.R.M. Ibrahim, G.A. Mohamed, Anti-quorum sensing activity of some medicinal plants, Afr. J. Tradit. Complement. Altern. Med. 13 (2016) 67–71.
[14] K. Bacha, Y. Tariku, F. Gebreyesus, S. Zerihun, A. Mohammed, N. Weiland-Bräuer, R.A. Schmitz, M. Mulat, Antimicrobial and anti-quorum sensing activities of selected medicinal plants of Ethiopia: implication for development of potent antimicrobial agents, BMC Microbiol. 16 (2016) 139, https://doi.org/10.1186/s12866-016-0765-9.
[15] C.L. Chaffer, R.A. Weinberg, A perspective on cancer cell metastasis, Science 331 (2011) 1559–1564.
[16] M.K. Kathiravan, M.M. Khilare, K. Nikoomanesh, A.S. Chothe, K.S. Jain, Topoisomerase as target for antibacterial and anticancer drug discovery, J. Enzyme Inhib. Med. Chem. 28 (2013) 419–435.
[17] J.A.W. Byl, S.D. Cline, T. Utsugi, T. Kobunai, Y. Yamada, N. Osheroff, DNA topoisomerase II as the target for the anticancer drug TOP-53: mechanistic basis for drug action, Biochemistry 40 (2001) 712–718.
[18] C.C. Wu, T.K. Li, L. Farh, L.Y. Lin, T.S. Lin, Y.J. Yu, T.J. Yen, C.W. Chian, Structural basis of type II topoisomerase inhibition by the anticancer drug etoposide, Science 333 (2011) 459–462.
[19] M.S. Salem, M.A.M. Ali, Novel pyrazolo[3,4-*b*]pyridine derivatives: synthesis, characterization, antimicrobial and antiproliferative profile, Biol. Pharm. Bull. 39 (2016) 473–483.
[20] M.A. El-Borai, H.F. Rizk, D.M. Beltagy, I.Y. El-Deeb, Microwave-assisted synthesis of some new pyrazolopyridines and their antioxidant, antitumor and antimicrobial activities, Eur. J. Med. Chem. 66 (2013) 415–422.
[21] M.A.A. El-Remaily, O.M. El Hady, H.S. Abo Zaid, E.M.M. Abd El-Raheem, Synthesis and *in vitro* antibacterial activity of some novel fused pyridopyrimidine derivatives, J. Heterocycl. Chem. 53 (2016) 1304–1309.
[22] W.S. Hamama, H.G. El-Gohary, M. Soliman, H.H. Zoorob, A versatile synthesis, PM3-semiempirical, antibacterial, and antitumor evaluation of some bioactive pyrazoles, J. Heterocycl. Chem. 49 (2012) 543–554.
[23] A. Bazgir, M.M. Khanaposhtani, A.A. Soorki, One-pot synthesis and antibacterial activities of pyrazolo[4′,3′:5,6]pyrido[2,3-*d*]pyrimidine-dione derivatives, Bioorg. Med. Chem. Lett. 18 (2008) 5800–5803.
[24] P. Acosta, B. Insuasty, A. Ortiz, R. Abonia, M. Sortino, S.A. Zacchino, J. Quirog, Solvent-free microwave-assisted synthesis of novel pyrazolo[4́,3́:5,6]pyrido[2,3-*d*] pyrimidines with potential antifungal activity, Arab. J. Chem. 9 (2016) 481–492.
[25] M.A. El-Hashash, S.M. Sherif, A.A.E. Badawy, H.R.M. Rashdan, Facial synthesis of some new pyrazolopyridine, barbituric and thiobarbituric acid derivatives with antimicrobial activities, Int. J. Adv. Res. 2 (2014) 900–913.
[26] T.I. El-Emary, S.A. Abd, El-Mohsen, Multi-component one-pot synthesis and antimicrobial activities of 3-methyl-1,4-diphenyl-7-thioxo-4,6,8,9-tetrahydropyrazolo [5,4-*b*]pyrimidino[5,4-*e*]pyridine-5-one and related derivatives, Molecules 17 (2012) 14464–14483.
[27] I.H. Eissa, A.M. El-Naggar, M.A. El-Hashash, Design, synthesis, molecular modeling and biological evaluation of novel 1*H*-pyrazolo[3,4-*b*]pyridine derivatives as potential anticancer agents, Bioorg. Chem. 67 (2016) 43–56.
[28] N.R. Mohamed, N.Y. Khaireldin, A.F. Fahmy, A.A. El-Sayed, Facile synthesis of fused nitrogen containing heterocycles as anticancer agents, Der Pharma Chem. 2 (1) (2010) 400–417.
[29] M.M. Mohamed, A.K. Khalil, E.M. Abbass, A.M. El-Naggar, Design, synthesis of new pyrimidine derivatives as anticancer and antimicrobial agents, Synth. Commun. 47 (2017) 1441–1457.
[30] N.U. Güzeldemirci, Ö. Küçükbasmacı, Synthesis and antimicrobial activity evaluation of new 1,2,4-triazoles and 1,3,4-thiadiazoles bearing imidazo[2,1-*b*]thiazole moiety, Eur. J. Med. Chem. 45 (2010) 63–68.
[31] K.F. Ansari, C. Lal, R.K. Khitoliya, Synthesis and biological activity of some triazole-bearing benzimidazole derivatives, J. Serb. Chem. Soc. 76 (2011) 341–352.
[32] K.S. Bhat, B. Poojary, D.J. Prasad, P. Naik, B.S. Holla, Synthesis and antitumor activity studies of some new fused 1,2,4-triazole derivatives carrying 2,4-dichloro-5-fluorophenyl moiety, Eur. J. Med. Chem. 44 (2009) 5066–5070.
[33] L.K. Gediya, V.C. Njar, Promise and challenges in drug discovery and development of hybrid anticancer drugs, Expert. Opin. Drug Discov. 4 (2009) 1099–1111.
[34] C.V. Junior, A. Danuello, V.dS. Bolzani, E.J. Barreiro, C.A.M. Fraga, Molecular hybridization: a useful tool in the design of new drug prototypes, Curr. Med. Chem. 14 (2007) 1829–1852.
[35] H.N. Hafez, A.G. Alshammari, A.-R.B.A. El-Gazzar, Facile heterocyclic synthesis and antimicrobial activity of polysubstituted and condensed pyrazolopyranopyrimidine and pyrazolopyranotriazine derivatives, Acta Pharm. 65 (2015) 399–412.
[36] N.S. El-Gohary, Synthesis and *in vitro* antitumor activity of new quinoline, pyrimido [4,5-*b*]quinoline, [1,2,3]triazino[4,5-*b*]quinoline, and [1,2,4]triazolo[2′,3′:3,4] pyrimido[6,5-*b*]quinoline analogs, Med. Chem. Res. 22 (2013) 5236–5247.
[37] L. Garutia, M. Roberti, T. Rossi, M. Castelli, M. Malagoli, Synthesis and antiproliferative activity of 3-substituted 1*H*-indole [3,2-*d*]1,2,3-triazin-4(3*H*)-ones, Eur. J. Med. Chem. 33 (1998) 43–46.
[38] C.J. Shishoo, M.B. Devani, G.V. Ullas, S. Ananthan, V.S. Bhadti, Studies on the synthesis of 2-(2-arylvinyl)thieno[2,3-*d*]pyrimidines and 5-(2-arylvinyl)triazolothieno[3,2-*e*]pyrimidines, J. Heterocycl. Chem. 22 (1985) 825–830.
[39] F.M. Abdelrazek, Heterocyclic synthesis with nitriles: synthesis of some new thiophene and thieno[2,3-*d*]pyrimidine derivatives, Phosphor. Sulfur Silicon Relat. Elem. 119 (1996) 271–277.
[40] Clinical Laboratory Standards Institute (CLSI), Performance Standards for Antimicrobial Susceptibility Testing; Twenty-Fifth Informational Supplement. Clinical and Laboratory Standards Institute, Wayne, PA, USA (2015) M100-S25.
[41] Clinical Laboratory Standards Institute (CLSI), Reference Method for Broth Dilution Antifungal Susceptibility Testing of Yeasts; Approved Standard-Third Edition. Clinical and Laboratory Standards Institute, Wayne, PA, USA (2008) M27-A3.
[42] Clinical Laboratory Standards Institute (CLSI), Reference Method for Broth Dilution Antifungal Susceptibility Testing of Filamentous Fungi; Approved Standard-Second Edition. Clinical and Laboratory Standards Institute, Wayne, PA, USA (2008) M38-A2.
[43] K.H. McClean, M.K. Winson, L. Fish, A. Taylor, S.R. Chhabra, M. Camara, M. Daykin, J.H. Lamb, S. Swift, B.W. Bycroft, G.S. Stewart, P. Williams, Quorum sensing and *Chromobacterium violaceum*: exploitation of violacein production and inhibition for the detection of *N*-acyl homoserine lactones, Microbiology 143 (1997) 3703–3711.
[44] T. Morohoshi, M. Kato, K. Fukamachi, N. Kato, T. Ikeda, *N*-acylhomoserine lactone regulates violacein production in *Chromobacterium violaceum* type strain ATCC 12472, FEMS Microbiol. Lett. 279 (2008) 124–130.
[45] G. Devescovi, M. Kojic, S. Covaceuszach, M. Cámara, P. Williams, I. Bertani, S. Subramoni, V. Venturi, Negative regulation of violacein biosynthesis in *Chromobacterium violaceum*, Front. Microbiol. 8 (2017) 349, https://doi.org/10.3389/fmicb.2017.00349.
[46] F. Denizot, R. Lang, Rapid colorimetric assay for cell growth and survival. Modifications to the tetrazolium dye procedure giving improved sensitivity and reliability, J. Immunol. Methods 89 (1986) 271–277.
[47] D. Gerlier, T. Thomasset, Use of MTT colorimetric assay to measure cell activation, J. Immunol. Methods 94 (1986) 57–63.
[48] T. Mosmann, Rapid colorimetric assay for cellular growth and survival: application to proliferation and cytotoxicity assays, J. Immunol. Methods 65 (1983) 55–63.
[49] C. Oberling, M. Guerin, The role of viruses in the production of cancer, Adv. Cancer Res. 2 (1954) 353–423.
[50] K.R. Sheeja, G. Kuttan, R. Kuttan, Cytotoxic and antitumour activity of Berberine, Amala Res. Bull. 17 (1997) 73–76.
[51] B.D. Clarkson, J.H. Burchenal, Preliminary screening of antineoplastic drugs, Prog.

Clin. Cancer 1 (1965) 625–629.
[52] P.G. Baraldi, A. Bovero, F. Fruttarolo, R. Romagnoli, DNA minor groove binders as potential antitumor and antimicrobial agents, Med. Res. Rev. 24 (2004) 475–528.
[53] N.S. Burres, A. Frigo, R.R. Rasmussen, J.B. McAlpine, A colorimetric microassay for the detection of agents that interact with DNA, J. Nat. Prod. 55 (1992) 1582–1587.
[54] N.A. Smith, J.A. Byl, S.L. Mercer, J.E. Deweese, N. Osheroff, Etoposide quinone is a covalent poison of human topoisomerase IIβ, Biochemistry 53 (2014) 3229–3236.
[55] X. Wang, K. Song, L. Li, L. Chen, Structure-based drug design strategies and challenges, Curr. Top. Med. Chem. 18 (2018) 998–1006.
[56] V. Lounnas, T. Ritschel, J. Kelder, R. McGuire, R.P. Bywater, N. Foloppe, Current progress in structure-based rational drug design marks a new mindset in drug discovery, Comput. Struct. Biotechnol. J. 5 (2013) e201302011, https://doi.org/10.5936/csbj.201302011.
[57] R.C. Wade, O.M.H. Salo-Ahen, Molecular modeling in drug design, Molecules 24 (2019) 321, https://doi.org/10.3390/molecules24020321.
[58] L.G. Ferreira, R.N. Dos Santos, G. Oliva, A.D. Andricopulo, Molecular docking and structure-based drug design strategies, Molecules 20 (2015) 13384–13421.
[59] E.F. Meyer, S.M. Swanson, J.A. Williams, Molecular modelling and drug design, Pharmacol. Ther. 85 (2000) 113–121.
[60] R. Thomsen, M.H. Christensen, MolDock: a new technique for high accuracy molecular docking, J. Med. Chem. 49 (2006) 3315–3321.
[61] LeadIT version 2.3.2; BioSolveIT GmbH, Sankt Augustin, Germany, 2017, www.biosolveit.de/LeadIT.
[62] G. Wolber, T. Langer, LigandScout: 3D Pharmacophores derived from protein bound ligands and their use as virtual screening filters, J. Chem. Inf. Model. 45 (2005) 160–169.
[63] R.U. Kadam, N. Roy, Recent trends in drug likeness prediction: a comprehensive review of *in silico* methods, Ind. J. Pharm. Sci. 69 (2007) 609–615.
[64] C.A. Lipinski, F. Lombardo, B.W. Dominy, P.J. Feeney, Experimental and computational approaches to estimate solubility and permeability in drug discovery and development settings, Adv. Drug Deliv. Rev. 46 (2001) 3–26.
[65] D.F. Veber, S.R. Johnson, H.Y. Cheng, B.R. Smith, K.W. Ward, K.D. Kopple, Molecular properties that influence the oral bioavailability of drug candidates, J. Med. Chem. 45 (2002) 2615–2623.
[66] https://www.molinspiration.com/cgi-bin/properties.
[67] https://preadmet.bmdrc.kr/toxicity/.
[68] https://molsoft.com/mprop/.
[69] A. Jarrahpour, J. Fathi, M. Mimouni, T.B. Hadda, J. Sheikh, Z.H. Chohan, A. Parvez, Petra, Osiris and molinspiration (POM) together as a successful support in drug design: antibacterial activity and biopharmaceutical characterization of some azo Schiff bases, Med. Chem. Res. 21 (2012) 1984–1990.
[70] Z. Khiati, A.A. Othman, B. Guessas, Synthesis and antibacterial activity of 1,3,4-oxadiazole and 1,2,4-triazole derivatives of salicylic acid and its synthetic intermediates, S. Afr. J. Chem. 60 (2007) 20–24.
[71] C. Kus, G. Ayhan-Kilcigil, S. Ozbey, F.B. Kaynak, M. Kaya, T. Coban, B. Can-Eke, Synthesis and antioxidant properties of novel *N*-methyl-1,3,4-thiadiazol-2-amine and 4-methyl-2*H*-1,2,4-triazole-3(4*H*)-thione derivatives of benzimidazole class, Bioorg. Med. Chem. 16 (2008) 4294–4303.